Springer Praxis Books

Information Technologies for Remote Monitoring of the Environment

Bearbeitet von
Vladimir F. Krapivin, Anatolij M. Shutko

1. Auflage 2012. Buch. xxxiv, 502 S. Hardcover
ISBN 978 3 642 20566 8
Format (B x L): 16,8 x 24 cm
Gewicht: 1049 g

2

Survivability and biocomplexity

2.1 INTRODUCTION

One of the main problems facing modern science is the estimation of biosphere survivability under conditions of increasing anthropogenic impact. Such estimation can be brought about by using a biosphere model. Well-known attempts at synthesizing a global model have given unsatisfactory results. The global models that have been created are educational in nature and are not fit for purpose for real estimations. In the last couple of decades many investigators proposed creating reliable and effective systems that are capable of considering the environmental state globally. Generally, this proposal included developing technical means for the collection, storage, and transfer of the data on nature's state, on the one hand, and the development of methods to process these data, on the other hand. Current means for collecting information about natural objects and processes make it possible to form a dataset covering large territories—even the whole biosphere. Remote means of environmental monitoring have become especially effective. The aim of this chapter is to formulate a basic model of biosphere survivability and to propose a new view on global modeling. The behavior of any system is determined by the value it can place on the different terms characterizing the state of the system. By interacting with an external medium and, in particular, with other systems, the values of these terms can vary in one way or another. For any technological or biological system it must always be possible to show changes in the field of characteristic parameters in which the system can be considered to be functioning. Outside this field the system does not exist.

Thus, we can substitute the complex behavior of a system by describing the behavior depicting this system as a point in phase space of the characteristic parameters. If a change in any coordinate leads to the disappearance of the depicting point from the allowable field, the system collapses (i.e., the organism as a whole perishes).

V.F. Krapivin and A.M. Shutko, *Information Technologies for Remote Monitoring of the Environment*, Springer Praxis Books, DOI 10.1007/978-3-642-20567-5_2, © Springer-Verlag Berlin Heidelberg 2012

Significant variables are not identical regarding the degree of threat they pose to the system. Such variables as the oxygen content of blood or the structural integrity of the medulla oblongata cannot tolerate any significant changes, since such changes would almost invariably lead to immediate death. However, there are changes, such as in the temperature of individual areas of the skin where sharp fluctuations do not necessarily lead to such an eventuality. Separating all variables characterizing the state of the system into significant variables makes it possible to simplify the behavioral strategy of a system as it interacts with an external environment or other systems.

A system is defined by its structure and behavior. The behavior of such a system is aimed at providing uninterrupted functioning by means of a correspondingly organized structure and behavior. The characteristic of a complex system to actively withstand the hostile action of an external medium is referred to in this book as "survivability" (Abrahamson, 1989; Corcoran, 2005; EPA, 2005; Fleishman, 1965; Kondratyev *et al.*, 2003d; Krapivin, 1978; Krapivin and Nazaryan, 1995; Starke, 2004; Svirezhev, 1987; Tait, 1987).

In the present chapter an analysis is made of a system whose elements are subdivided into working, defending, and active external agents of the system, which suppress or neutralize the hostile actions of an external medium. By taking into account the possibility of suppressing the hostile action of an external medium and the vulnerability of all the elements of the system, it becomes possible to reach a theoretical game definition of the problems. The use of game theory to investigate the survivability of complex systems makes it possible to classify the most unfavorable action of an external medium on the system and to work out the best strategy behavior for the system. This study of antagonistic situations between systems enables the mechanisms involved in the adaptability of living systems to the varying conditions of an external medium to be understood.

2.2 PRINCIPAL DEFINITIONS

The biosphere is a complex unique system. Looked at historically, humankind was but an element of the biosphere. However, at the present time the problem of coevolution between human society (H) and nature (N) has arisen. The influence of human activity on natural systems has reached global scales, but it is still possible to divide anthropogenic and natural processes conditionally. The use of system analysis permits carrying out a more formal description of this division. There are commonly two interacting systems:

- H deals with technologies, sciences, economics, sociology, agriculture, industry, etc.;
- N deals with climatic, biogeocenotic, biogeochemical, hydrological, geophysical, and other natural processes.

Practical problems when investigating complex systems involve evaluating their effectiveness and, in particular, their stability under the indeterminate con-

ditions in which they function. The theory of the potential effectiveness of complex systems is used to resolve these problems (Fleishman, 1970). A constructive mathematical apparatus making it possible to solve the different problems that arise when optimizing the structure and behavior of H and N functioning in certain situations has been developed within the framework of this theory.

The systems H and N are determined by their structure (i.e., the number of elements and relations among them) and behavior (responses to impacts). The internal behavior of such a system is aimed at maintaining its uninterrupted functioning. The external behavior of the system is aimed at achieving a certain outside goal. The temporal stability of a complex system is a necessary property without which all its other properties become meaningless. This is connected with the structural stability of the material composition and energy balance of the complex system as well as with the regularity of its responses to the same external impacts.

A breach in the stability of a system may result from internal causes (the aging of its elements) or external causes associated with the unfavorable influence of the environment (an ill-intentioned enemy, in particular). The survivability of biological systems is determined by the environmental conditions that apply to them, humankind's interference with nature being an important factor. Keeping this in mind when trying to construct artificial biological systems leads to the problem of finding the best way to do this, increase in the productivity of a biological system being the main optimality criterion.

On the global scale, the problem of interacting system survivability is complicated by a hierarchy of interaction levels. For a complete explanation of H and N systems their openness has to be taken into account. It is normal to consider the interaction of two open complex systems H and N as defined by their goals H_G and N_G, structures H_S and N_S, and behavior H_B and N_B, respectively. Fleishman (1970) suggested that the functioning of such systems should be described by the equations involved in (V, W) exchange. In other words, the interaction of an open system with the environment (or other system) is represented as a process whereby the system exchanges a certain quantity V of resources spent in exchange for a certain quantity W of resources consumed. The aim of the systems is the most advantageous (V, W) exchange (i.e., it tries to get maximum W in exchange for minimum V). V is a complex function of the structure and behavior of both systems:

$$V = V(W, H_S, N_S, H_G, N_G) = V(W, H, N). \tag{2.1}$$

As a result of interaction, the systems H and N get the following (V, W) exchanges:

$$\left.\begin{aligned} V_{H,\max} &= V_{H,\max}(W_H, H^*, N^*) = \max_{\{H_B,H_S\}} \min_{\{N_B,N_S\}} V_H(W_H, H, N), \\ V_{N,\max} &= V_{N,\max}(W_N, H^*, N^*) = \max_{\{N_B,N_S\}} \min_{\{H_B,H_S\}} V_N(W_N, H, N), \end{aligned}\right\} \tag{2.2}$$

where H^* and N^* are the optimal H and N systems, respectively.

From equations (2.1) and (2.2) we can see that the value of (V, W) exchange depends on the goal of the system and may vary within certain limits: $V_{1,\min} \le V_H \le V_{1,\max}$, $V_{2,\min} \le V_N \le V_{2,\max}$, where $V_{i,\min}$ $(i = 1, 2)$ corresponds to the case when both systems are most aggressive, and $V_{i,\max}$ $(i = 1, 2)$ to the case when they are most cautious. In a word there is a *spectrum* of interactions between H and N. For a formal description of these interactions we shall divide all the elements of both systems into three classes: the working (functioning), protective (defensive), and active elements, the latter designed to act on the environment. In short, we shall refer to the working elements of systems H and N as a and b elements, to the protective elements as R_a and R_b elements, and to the active elements as C_a and C_b elements, respectively.

Let us assume that before interaction the systems H and N have certain limited energy resources (i.e., vital "substrates") V_a and V_b, where $V_a = \{V_{aj}, j = 1, \ldots, m_a\}$, $V_b = \{V_{bi}, i = 1, \ldots, m_b\}$. These substrates generate working elements in such a way that the substrate V_{aj} (V_{bi}) can generate H_j (N_i) a (b) elements of the jth $(i$th) type of values a_j (b_i).

The protective and active elements of each system are generated by the working elements. First of all, the protective E^a_{Rm} (E^b_{Rm}) and active E^a_{Cm} (E^b_{Cm}) substrates are created which, in their turn, generate R and C elements of the mth type. These processes are described by the following dependences:

$$E^a_{Rm} = E^a_{Rm}(V_a, H_1, \ldots, H_{m_a}) = \sum_{j=1}^{m_a} w^a_{mj} f^a_{jR}(V_{aj}, H_j),$$

$$E^b_{Rm} = E^b_{Rm}(V_b, N_1, \ldots, N_{m_b}) = \sum_{j=1}^{m_b} w^b_{mj} f^b_{jR}(V_{bj}, N_j),$$

$$E^a_{Cm} = E^a_{Cm}(V_a, H_1, \ldots, H_{m_a}) = \sum_{j=1}^{m_a} w'^a_{mj} f^a_{jC}(V_{aj}, H_j),$$

$$E^b_{Cm} = E^b_{Cm}(V_b, N_1, \ldots, N_{m_b}) = \sum_{j=1}^{m_b} w^b_{mj} f^b_{jC}(V_{bj}, N_j),$$

where $w^{a(b)}_{mj}$, $w'^{a(b)}_{mj}$, and $f^{a(b)}$ are current weights and functions, respectively.

Let us assume that, as a result of such hierarchical synthesis, elements in the systems H and N have at the beginning of the interaction (i.e., $t = 0$):

(1) m_j and n_j working elements of the jth type with values a_j and b_j, respectively, where

$$\sum_{j=1}^{m_a} a_j H_j = M_a(0), \qquad \sum_{j=1}^{m_b} b_j N_j = M_b(0); \tag{2.3}$$

(2) r_a and r_b types of protective elements, the mth type having α_m and β_m elements, and

$$\sum_{m=1}^{r_a} \alpha_m = M_{R_a}(0), \qquad \sum_{m=1}^{r_b} \beta_m = M_{R_b}(0); \tag{2.4}$$

(3) s_a and s_b types of active elements, the mth type having ν_m^a and ν_m^b elements, and

$$\sum_{m=1}^{s_a} \nu_m^a = D_a(0), \qquad \sum_{m=1}^{s_b} \nu_m^b = D_b(0); \tag{2.5}$$

respectively.

In the discrete case, change in the average number of system elements that have survived until moment t_{i+1} will be described by the following relations:

$$H_s(t_{i+1}) = \max\{0, H_s(t_i) - \sigma_{hs}^n(t_i) p_{hs}^n(t_i)\}, \qquad s = 1, \ldots, m_h \tag{2.6}$$

$$\alpha_j(t_{i+1}) = \max\{0, \alpha_j(t_i) - \sigma_{Rj}^n(t_i) p_{Rj}^n(t_i)\}, \qquad j = 1, \ldots, r_h \tag{2.7}$$

$$\nu_m^h(t_{i+1}) = \max\{0, \nu_m^h(t_i) - \sigma_{Cm}^n(t_i) p_{Cm}^n(t_i)\}, \quad m = 1, \ldots, s_h \tag{2.8}$$

$$N_l(t_{i+1}) = \max\{0, N_l(t_i) - \sigma_{nl}^h(t_i) p_{nl}^h(t_i)\}, \qquad l = 1, \ldots, m_n \tag{2.9}$$

$$\beta_s(t_{i+1}) = \max\{0, \beta_s(t_i) - \sigma_{Rs}^h(t_i) p_{Rs}^h(t_i)\}, \qquad s = 1, \ldots, r_n \tag{2.10}$$

$$\nu_m^n(t_{i+1}) = \max\{0, \nu_m^n(t_i) - \sigma_{Cm}^h(t_i) p_{Cm}^h(t_i)\}, \quad m = 1, \ldots, s_h, \tag{2.11}$$

where the $\sigma_{\omega i}^{a(b)}(t)$ values characterize the external behavior of both these systems:

$$\bar{H}_e^{(i)} = \{\|\sigma_{bl}^a\|, \|\sigma_{Rs}^a\|\}, \qquad \bar{N}_e^{(i)} = \{\|\sigma_{as}^b\|, \|\sigma_{Rj}^b\|\};$$

and $p_{\omega i}^{a(b)}(t)$ are the respective probabilities of death of the elements as a result of their interaction.

The following limiting conditions should be taken into account here:

$$\sum_{i=0}^{T} \left\{ \sigma_{Cs}^b(t_i) p_{Cs}^b(t_i) + \sum_{j=1}^{m_b} \sigma_{bj}^a(t_i) + \sum_{j=1}^{r_b} \sigma_{Rj}^a(t_i) + \sum_{j=1}^{s_b} \sigma_{Cj}^a(t_i) \right\} = \nu_l^h(0), \tag{2.12}$$

$$\sum_{i=0}^{T} \left\{ \sigma_{Cs}^a(t_i) p_{Cs}^a(t_i) + \sum_{j=1}^{m_a} \sigma_{aj}^b(t_i) + \sum_{j=1}^{r_a} \sigma_{Rj}^b(t_i) + \sum_{j=1}^{s_a} \sigma_{Cj}^b(t_i) \right\} = \nu_l^n(0). \tag{2.13}$$

The stochastic solution of equations (2.1)–(2.13) can be in the unrealized form in practice. There are many real situations when the realization of H^* or N^* system is impossible. Some tasks and algorithms were described by Krapivin and Klimov (1995, 1997).

2.3 SURVIVABILITY MODEL

Let us consider the interaction of the two systems within the framework of the diagram shown in Figure 2.1. At the start, systems H and N have, respectively, $N_a(0)$ and $N_b(0)$ working elements, $N_{Ra}(0)$ and $N_{Rb}(0)$ protective elements, and $M_a(0)$ and $M_b(0)$ active agents for undertaking action against an external medium. In this case we shall assume that the initial structures H_S and N_S of the systems are uniformly filled with elements. This means that at time $t = 0$ in any sphere with a fixed radius ε, which is completely confined within system H, there are constant numbers of elements.

We shall consider that all elements of systems H and N, independent of their spatial location, are accessible to the same degree to active agents of the external medium. The interaction of the systems consists in the situation in which each system in a fixed interval of time $[0, T]$ at discrete moments $t_i = ih$, $i = 0, 1, 2, \ldots, k$ $(k = [T/h])$ can determine its behavior by a set of numbers:

$$H_B = \{m_b(t_i), m_{Rb}(t_i), \rho_i\}, \qquad N_B = \{m_a(t_i), m_{Ra}(t_i), r_i\},$$

where m_a and m_b are parts of those C_b and C_a elements aimed at destroying a and b elements, respectively; analogously, parts $(1 - r_i)m_{Ra}$ and $(1 - \rho_i)m_{Rb}$ of C_b and C_a elements are directed at destroying the corresponding protective elements. In the course of time portions of C_a and C_b elements uniformly fill the opposite system, and in this way the elements of the systems become with time *uniformly depleted*.

It is assumed that system $H(N)$ is put out of operation if at time $t_i \leq T$, $N_a(t_i) \leq \theta_a N_a(0)$ $(N_b(t_i) \leq \theta_b N_b(0))$; that is, if more than the $(1 - \theta_a)$th $((1 - \theta_b)$th)

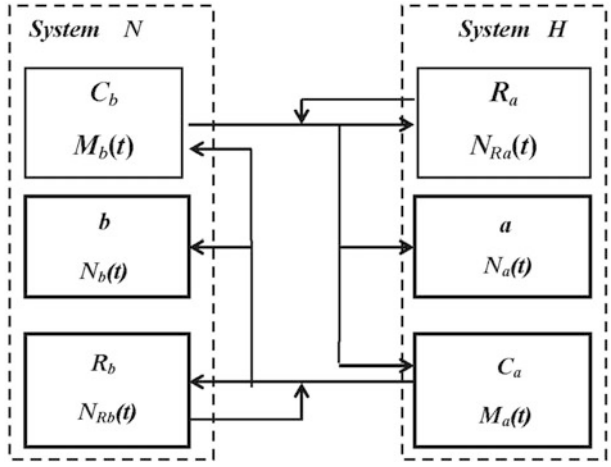

Figure 2.1. Schematic diagram of the interaction between two systems in the survivability problem (Kondratyev *et al.*, 2002).

portion of the initial number of its working elements is out of operation, where $0 \leq \theta_a, \theta_b \leq 1$. On the other hand, when $N_a(T) > \theta_a N_a(0)$ ($N_b(T) > \theta_b N_b(0)$), then system $H(N)$ is considered to have survived. The assignment of values θ_a and θ_b is determined by the peculiarities of the system under consideration. It is clear that the smaller the number θ, the more *survivable* the system.

Further, we shall assume that one of the elements of system H or N is put of operation by the action of one of the elements C_a or C_b with a probability $p_1[N_{Ra}(t)]$ or $p_2[N_{Rb}(t)]$, respectively. Consequently, in the interval of time $[t_i, t_i + h]$ with step length h there occur on average the following changes in the structure of the system:

$$\left.\begin{aligned}
N_a(t_i) - N_a(t_i + h) &= m_a(t_i)p_1[N_{Ra}(t_i)], \\
M_a(t_i) - M_a(t_i + h) &= r_i m_{Ra}(t_i)[N_{Ra}(t_i) + m_b(t_i) + m_{Rb}(t_i), \\
N_{Ra}(t_i) - N_{Ra}(t_i + h) &= (1 - r_i)m_{Ra}(t_i)p_1[N_{Ra}(t_i)], \\
N_b(t_i) - N_b(t_i + h) &= m_b(t_i)p_2[N_{Rb}(t_i)], \\
M_b(t_i) - M_b(t_i + h) &= \rho_i m_{Rb}(t_i)p_2[N_{Rb}(t_i)] + m_a(t_i) + m_{Ra}(t_i), \\
N_{Rb}(t_i) - N_{Rb}(t_i + h) &= (1 - \rho_i)m_{Rb}(t_i)p_2[N_{Rb}(t_i)].
\end{aligned}\right\} \tag{2.14}$$

The above-discussed interaction scheme of the two systems can be readily implemented using game theory methods. Indeed, from equations (2.14) it follows that in the interval of time $[0, T]$ ($T = kh$, we can take $h = 1$ here) both systems lose working a and b elements in the following amounts:

$$Q_1 = \sum_{n=0}^{k-1} m_a(n)p_1[N_{Ra}(n)], \qquad Q_2 = \sum_{n=0}^{k-1} m_b(n)p_2[N_{Rb}(n)]. \tag{2.15}$$

In this case, system H with its behavior of $H_B(t) = \{m_b(t), m_{Rb}(t), \rho(t)\}$ tends to minimize the function Q_1 (which characterizes its losses) and to maximize Q_2 (the losses of system N). On the other hand, system N with its behavior $N_B(t) = \{m_a(t), m_{Ra}(t), r(t)\}$ tends to maximize function Q_1 and minimize function Q_2.

In practical problems, the win function is taken as that characteristic of the antagonistic situation that describes a given conflict most fully. In this case such a function is $Q = Q_1 - Q_2$. The maximizing participant in this case will be system N, the minimizing opponent system H. In this manner, solution of the set problem on the optimal behavior of the two systems in an antagonistic situation is reduced to solution of a game with a win function:

$$Q(H_B, N_B) = \sum_{n=0}^{i-1} \{m_a(n)p_1[N_{Ra}(n)] - m_b(n)p_2 N_{Rb}(n)]\}, \tag{2.16}$$

where, according to equation (2.14),

$$\left.\begin{aligned} N_{Ra}(n) &= N_{Ra}(0) - \sum_{i=0}^{n-1}(1-r_i)m_{Ra}(i)p_1[N_{Ra}(i)], \\ N_{Rb}(n) &= N_{Rb}(0) - \sum_{i=0}^{n-1}(1-\rho_i)m_{Rb}(i)p_{21}[N_{Rb}(i)], \end{aligned}\right\} \tag{2.17}$$

and conditions are imposed on the behavior of the system related to limitations of the C_a and C_b elements:

$$\left.\begin{aligned} \sum_{i=0}^{k-1}\{r_i m_{Ra}(i)p_1[N_{Ra}(i)] + m_b(i) + m_{Rb}(i)\} &= M_a(0), \\ \sum_{i=0}^{k-1}\{\rho_i m_{Rb}(i)p_2[N_{Rb}(i)] + m_a(i) + m_{Ra}(i)\} &= M_b(0). \end{aligned}\right\} \tag{2.18}$$

Thus, we have a k-step survival game. At the start of each step, system H provides a certain amount of its resources $u = \{m_b, m_{Rb}, \rho\}$ and N provides a certain amount of its resources $v = \{m_a, m_{Ra}, r\}$, so that limitations (2.18) are maintained. As a result of this distribution of resources, system N gets the advantage:

$$R(u, v, M_a, M_b) = m_a p_1[N_{Ra}]. \tag{2.19}$$

However, N's win and H's losses are not counted on the basis of their initial resources and cannot be added to the remaining amounts of C elements. After each step of the game (equation 2.14), a change in the resources available to the participants takes place, and as a result of the k-step process the total win of system N can be described by the equation:

$$\begin{aligned} Q_k &= Q_k[u_0, u_1, \ldots, u_{k-1}; v_0, v_1, \ldots, v_{k-1}; M_a(0), M_b(0)] \\ &= \sum_{n=0}^{k-1}\{m_a(n)p_1[N_{Ra}(n)] - m_b(n)p_2[N_{Rb}(n)]\}. \end{aligned} \tag{2.20}$$

There are several methods that can help analyze this k-step process. One can consider this k-step game as a one-step game, in which case system H must select simultaneously a plurality of the vector $\{u_0, u_1, \ldots, u_{k-1}\}$, and system N a plurality of the vector $\{v_0, v_1, \ldots, v_{k-1}\}$, where the selection of u_k and v_k depends on the previous values obtained according to equation (2.14).

To solve this complex problem, we suggest substituting it by the similar problem of multi-step optimization. The values of this game can be expressed as:

$$\begin{aligned} V_k &= \max_F \min_G \left\{ \int Q_k \, dF(v_0, v_1, \ldots, v_{k-1}) \, dG(u_0, u_1, \ldots, u_{k-1}) \right\} \\ &= \min_G \max_F \{\cdots\} \end{aligned} \tag{2.21}$$

where the distribution functions F and G are determined on the boundaries of the complex form:

$$\begin{aligned} 0 \le v_0 \le M_b(0) \qquad & 0 \le u_0 \le M_a(0) \\ 0 \le v_1 \le M_b(1) \qquad & 0 \le u_1 \le M_a(1) \\ \vdots \qquad & \vdots \\ 0 \le v_{k-1} \le M_b(k-1) \qquad & 0 \le u_{k-1} \le M_a(k-1). \end{aligned} \tag{2.22}$$

By utilizing the optimality principle and taking into account the dependence $V_k = V_k[M_a(0), M_b(0)]$, we obtain the following functional equation:

$$\begin{aligned} & V_{n+1}[M_a(0), M_b(0)] \\ & = \max_F \min_G \left[\int\int_{\substack{0 \le u \le M_a(n-1) \\ 0 \le v \le M_b(n-1)}} \{R(u,v) + V_n[M_a(n-1), M_b(n-1)]\}\, dF(v)\, dG(u) \right] \\ & = \min_G \max_F [\cdots] \end{aligned} \tag{2.23}$$

where

$$\begin{aligned} V_1[M_a(0), M_b(0)] &= \max_F \min_G \left[\int\int_{\substack{0 \le u \le M_a(0) \\ 0 \le v \le M_b(0)}} R(u,v)\, dF(v)\, dG(u) \right] \\ &= \min_G \max_F [\cdots]. \end{aligned} \tag{2.24}$$

Finding a solution to these functional equations is difficult. This was the reason that the so-called *curse of dimensionality* was introduced. In this chapter we shall present the solution to some specific cases. However, this is carried out in more detail by Nitu *et al.* (2000a). To solve the proposed problem, we shall begin with a case where the C and R elements are indistinguishable in both systems. A diagram of the interaction between systems H and N is shown in Figure 2.2. By taking into account the designations used in this diagram, we obtain the number of C_a and C_b elements that have reached the C_b and C_a elements of the opposite system in a one-step operation. They are, respectively, $\max\{0, a_C - N_{Rb}\}$ and $\max\{0, b_C - N_{Ra}\}$. Therefore, the numbers of C_a and C_b elements that are put out of operation on average are $\max\{0, b_C - N_{Ra}\}p_1[N_{Ra}]$ and $\max\{0, a_C - N_{Rb}\}p_2[N_{Rb}]$. Consequently, after one step of the game there remain in the system the following numbers of C_a and C_b elements that are not put out of operation: $\max[0, M_a - \max(0, b_C - N_{Ra})p_1[N_{Ra}]]p_1[N_{Ra}]$ and $\max[0, M_b - \max(0, a_C - N_{Rb})p_2[N_{Rb}]]p_2[N_{Rb}]$. Turning to the multi-step situation, we introduce the win function (2.16). The aim of system N is to destroy system H or, more precisely, to put all of the latter's a elements out of operation. For this purpose system N cannot use all its C_b elements, since it will then be left defenseless against the C_a elements. An analogous situation holds true for system H. After each successive step of the game each system is compelled to release a

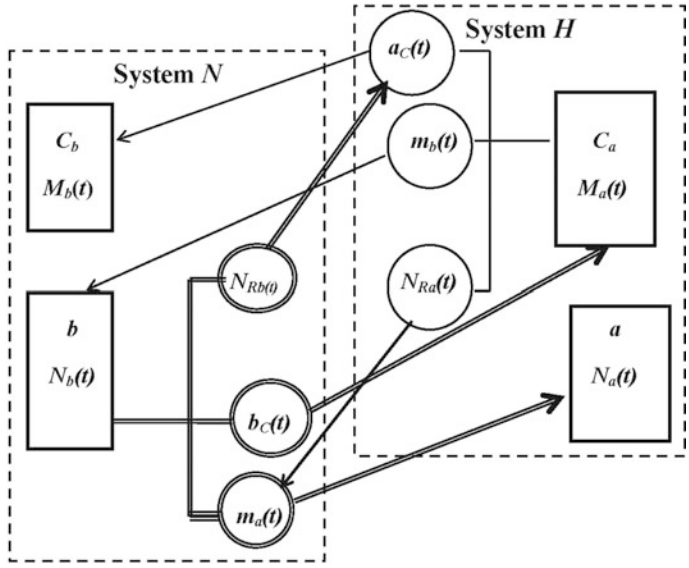

Figure 2.2. Schematic diagram of mutual interchangeability.

certain number of working a and b elements. The magnitude of this payoff is proportional to the difference $M_b - b_C - N_{Rb} - (M_a - a_C - N_{Ra})$. Now the problems on both sides become clear. System N must strive to provide such a number of C_b elements in all directions so as to maintain the maximum value of this difference. That is, it must provide the largest possible number of elements m_a for the destruction of a elements and thus increase its winnings. However, we shall also consider the presence of an analogous distribution of C_a elements and provide sufficient protection for system N through the maximum distribution of C_a elements. An analogous situation exists for system H. For the $(n-1)$ moves that remain before the end of the game, we have:

$$\left.\begin{aligned} M_a(n-1) &= \max\{0, M_a(n) - \max[0, b_C(n) - N_{Ra}(n)p_1[N_{Ra}(n)]\}p_1[N_{Ra}(n)], \\ M_b(n-1) &= \max\{0, M_b(n) - \max[0, a_C(n) - N_{Rb}(n)]p_2[N_{Rb}(n)]\}p_2[N_{Rb}(n)]. \end{aligned}\right\} \quad (2.25)$$

The payoff for the entire game according to equation (2.20) will be:

$$Q_k = \sum_{n=1}^{k}\{M_b(n) - b_C(n) - N_{Rb}(n) - [M_a(n) - a_C(n) - N_{Ra}(n)]\}. \quad (2.26)$$

The functional equation (2.23) will acquire the following form:

$$\begin{aligned} V_{n+1} &= \max_{H_B}\min_{N_B}\{M_b(n+1) - b_C(n+1) - N_{Rb}(n+1) - [M_a(n+1) - a_C(n+1) \\ &\quad - N_{Ra}(n+1)] + Q_k[M_a(n), M_b(n)]\} \\ &= \min_{N_B}\max_{H_B}\{\cdots\}. \end{aligned} \quad (2.27)$$

Since at the end of the game $Q_0 = 0$, we obtain from equation (2.26) for $k = 1$:

$$Q_1 = M_b(1) - b_C(1) - N_{Rb}(1) - M_a(1) + a_C(1) + N_{Ra}(1). \tag{2.28}$$

From equation (2.28), one step before the end of the game, we obtain the following optimal strategies:

$$N_{Rb}(1) = N_{Ra}(1) = 0, \qquad a_C(1) = b_C(1) = 0 \tag{2.29}$$

and the prize of the game is $V_1 = M_b(1) - M_a(1)$. This means that in the last step of the game both systems direct all their C_a and C_b elements that have remained from the previous steps towards the destruction of b and a elements, respectively. Analogously, two steps before the end of the game, we have:

$$Q_2 = M_b(2) - M_a(2) + a_C(2) - b_C(2) + N_{Ra}(2) - N_{Rb}(2) + V_1[M_a(1), M_b(1)] \tag{2.30}$$

where $V_1 = M_b(1) - M_a(1)$; and

$$\left.\begin{aligned} M_a(1) &= \max\{0, M_a(2) - \max[0, b_C(2) - N_{Ra}(2)]p_1[N_{Ra}(2)]\}p_1[N_{Ra}(2)], \\ M_b(1) &= \max\{0, M_b(2) - \max[0, a_C(2) - N_{Rb}(2)]p_2[N_{Rb}(2)]p_2[N_{Rb}(2)]. \end{aligned}\right\} \tag{2.31}$$

It is obvious at this step of the game that the participants have no pure strategies. Therefore, solution of this game is impossible analytically, and it can only be obtained in a concrete case by the numerical method. Modeling of the game provides some understanding of the nature of its solution. Indeed, with the aid of a computer it is possible either to construct a model of the game and to gather statistics or to solve the functional equation (2.23) numerically and, with the aid of heuristic concepts, to investigate the dependence of strategies on the initial conditions. Of course, such an approach for a short interval of modeling cannot give any significant information concerning the solution. Nevertheless, this is the only possible approach at the present time. The feeling of hopelessness in a specific situation should not deter us from seeking a solution by analytical methods. The importance of obtaining analytical solutions is obvious, since they have an advantage over numerical solutions in that they make possible the detection of general regularities of the optimal behavior of complex systems in antagonistic situations. The importance of analytical solutions was pointed out by Krapivin (1978), who showed that a single numerical solution cannot replace an analytical solution in which the quantitative description of the phenomenon is most concentrated. In the case examined here, when the participants have no information concerning the action of the opponent in the process of the entire game, the solution of particular cases with the aid of a computer enables us to obtain the following quantitative description of optimal strategies.

Let $M_b(n)/M_a(n) = \delta_n$. Then if $\delta_n \gg 1$, system N in the initial stage of the game has a pure strategy, but it is more advantageous for system H to adopt a mixed strategy, using the tactics of deception. During the first steps, system N destroys only C_a elements and it is only during the last steps that it destroys a elements. By using the corresponding probability mechanism, system H must direct all its C_a elements with probability p_1 towards the destruction of C_b elements, with probability p_2 towards the defense of its own elements, and with

probability $1 - p_1 - p_2$ towards the attack of b elements. In the case when $\delta_n \cong 1$, then at this stage of the game $p_1 + p_2 = 1$, $m_b(n) = 0$, and the behavior of the system becomes symmetrical. During the last steps of the game systems H and N, independent of the magnitude of δ_n, change over to the strategies $m_a(t) \neq 0$, $m_b(t) \neq 0$, and $b_C = a_C = N_{Ra} = N_{Rb} = 0$ (i.e., to the destruction of working elements).

Let us consider a particular case where the systems have no protective elements (i.e., $N_{Ra} = N_{Rb} = 0$) and, therefore, $p_1 = p_2 = 1$. Then we obtain:

$$M_a(n-1) = \max\{0, M_a(n) - b_C(n)\}, \quad M_b(n-1) = \max\{0, M_b(n) - a_C(n)\}. \quad (2.32)$$

One step before the end of the game, the payoff according to equation (2.31) is $V_1 = M_b(1) - M_a(1)$ and the optimal strategies $a_C^*(1) = b_C^*(1) = 0$; that is, the systems release all their C elements in an attempt to destroy the a and b elements, respectively.

Next, by assuming $n = 2$, according to equations (2.30) and (2.31) we obtain:

$$Q_2[a_C(2), b_C(2)] = \begin{cases} Q_{21} & \text{when } b_C(2) \geq M_a(2), a_C(2) \geq M_b(2); \\ Q_{22} & \text{when } b_C(2) < M_a(2), a_C(2) \geq M_b(2); \\ Q_{23} & \text{when } b_C(2) \geq M_a(2), a_C(2) < M_b(2); \\ Q_{24} & \text{when } b_C(2) < M_a(2), a_C(2) < M_b(2), \end{cases} \quad (2.33)$$

where $Q_{21} = M_b(2) - b_C(2) - M_a(2) + a_C(2)$; $Q_{22} = M_b(2) - 2M_a(2) + a_C(2)$; $Q_{23} = 2M_b(2) - b_C(2) - M_a(2)$; and $Q_{24} = 2M_b(2) - 2M_a(2)$.

The solution to the game with the win function (2.33) has the following form:

$$V_2 = 2M_b(2) - 2M_a(2), \qquad b_C^*(2) = M_a(2); a_C^*(2) = M_b(2). \quad (2.34)$$

Actually, if account is made of the real situation, the optimal strategies of both systems two steps before the end of the game will be as follows:

$$a_C^*(2) = \min\{M_a(2), M_b(2)\}, \qquad b_C^*(2) = \min\{M_a(2), M_b(2)\}. \quad (2.35)$$

Therefore at the penultimate step when $\delta_2 > 1$, system N releases a portion of its force and system H releases all its forces against the c elements of the other system.

Through analogous reasoning, we can see that n steps before the end of the game the strategies of systems H and N will be:

$$a_C^*(n) = \min\{M_a(n), M_b(n)\}; \qquad b_C^*(n) = \min\{M_a(n), M_b(n)\}. \quad (2.36)$$

If in the process of the game C elements are clearly not replaced in systems H and N, then it follows from equations (2.35) and (2.36) that it makes sense to conduct the game in two steps; and the two following cases are distinguishable:

(1) when $M_a(0) = M_b(0)$, both systems release all their C elements into battle against the C elements of the other system, but in so doing the systems themselves survive;

(2) when $M_a(0) > M_b(0)$, system N releases all the elements into battle against C_a elements, and system H releases $M_b(0)$ of C_a elements into battle against C_b elements, and $M_a(0) - M_b(0)$ of C_a elements into battle against b elements. Consequently, system H survives in every case, while system N survives only when $M_a(0) - M_b(0) < \theta_b N_b(0)$.

Now, let us consider the case in which C_a and C_b elements are mutually indifferent. In this case, by supposing $r = \rho = 0$ in equations (2.17) and (2.18), we obtain:

$$\left.\begin{aligned} N_{Ra}(n) &= N_{Ra}(0) - \sum_{i=0}^{n-1} m_{Ra}(i) p_1[N_{Ra}(i)], \\ N_{Rb}(n) &= N_{Rb}(0) - \sum_{i=0}^{n-1} m_{Rb}(i) p_2[N_{Rb}(i)] \end{aligned}\right\} \tag{2.37}$$

and

$$\sum_{n=0}^{k-1} [m_a(n) + m_{Ra}(n)] = M_b(0), \qquad \sum_{n=0}^{k-1} [m_b(n) + m_{Rb}(n)] = M_a(0). \tag{2.38}$$

The solution to the game of the two systems, H and N, with the win function as shown in equation (2.16) and under conditions as expressed in equations (2.37) and (2.38), is reduced to the problem of maximizing two functions:

$$Q_1 = \sum_{n=0}^{k-1} m_a(n) p_1[N_{Ra}(n)] = \max_{Ra} \tag{2.39}$$

$$Q_2 = \sum_{n=0}^{k-1} m_b(n) p_2[N_{Rb}(n)] = \max_{Rb} \tag{2.40}$$

From equations (2.39) and (2.40) it is evident that the optimal strategies of both sides consist in destroying a and b elements when $p_1[N_{Ra}(n)] = p_2[N_{Rb}(n)] = 1$. If the C elements act independently of one another, and the probability of putting the C elements out of operation by a single R element is equal to a constant value D_a and D_b for the H and N systems, respectively, then

$$p_1[N_{Ra}(n)] = \exp[-d_a N_{Ra}(n)], \qquad p_2[N_{Rb}(n)] = \exp[-d_b N_{Rb}(n)], \tag{2.41}$$

where, $d_a = -\theta_1 \ln(1 - D_a)$, $d_b = -\theta_2 \ln(1 - D_b)$ are the *effectiveness* coefficients of the R_a and R_b elements; and θ_1 and θ_2 are the *density* of the location of elements in the H and N system, respectively.

When $k = 1$, the optimal strategies of the behavior of the systems will be $m_a^*(0) = M_b(0)$ and $m_b^*(0) = M_a(0)$. This is natural since in the last step it makes no sense to destroy protective elements. When $k = 2$, from equations (2.37)–(2.40)

we obtain the optimal strategies in the form:

$$\left.\begin{aligned} m_a^*(0) = m_b^*(0) = m_{Ra}^*(1) = m_{Rb}^*(1) = 0, \quad m_a^*(1) = d_a^{-1}\exp[d_a N_{Ra}(0)], \\ m_b^*(1) = d_b^{-1}\exp[d_b N_{Rb}(0)], \quad m_{Ra}(0) = M_b(0) - d_a^{-1}\exp[d_a N_{Ra}(0)], \\ m_{Rb}(0) = M_a(0) - d_b^{-1}\exp[b_b N_{Rb}(0)]. \end{aligned}\right\} \tag{2.42}$$

The cost of the game is:

$$V_2 = d_a^{-1}\exp\{-1 + d_a M_b(0)\exp[-d_a N_{Ra}(0)]\} - d_b^{-1}\exp\{-1 + d_b M_a(0)\exp[-d_b N_{Rb}(0)]\}. \tag{2.43}$$

From equation (2.43) it is evident that for system N to destroy system H it is necessary that the following inequality holds:

$$d_a M_b(0)\exp[-d_a N_{Ra}(0)] \geq l_n[d_a e(1-\theta_a)N_a(0)] \tag{2.44}$$

from which we have:

$$M_b(0) \geq d_a^{-1}\exp[d_a N_{Ra}(0)]\{1 + l_n[d_a(1-\theta_a)N_a(0)]\}. \tag{2.45}$$

Similarly, we obtain the condition for system H:

$$M_a(0) \geq d_b^{-1}\exp[d_b N_{Rb}(0)]\{1 + l_n[d_b(1-\theta_b)N_b(0)]\}. \tag{2.46}$$

Thus, for system N to destroy system H it is necessary that inequality (2.45) holds. Analogously, for system H it is necessary that inequality (2.46) holds. The number of a and b elements, as a rule, is fixed, as follows from considerations related to the work of the system. The number of R elements, which perform protective functions, can be best selected when certain physical parameters in the problem are fixed and when *a priori* information concerning the number of C elements of the opposite system is available. For example, if the effectiveness of all R elements is constant independent of their number, then in order for system H to survive, the necessary number of protective elements must satisfy the inequality:

$$N_{Ra}(0) \geq d_a M_b(0) l_n / \{d_a(1 + l_n[d_a(1-\theta_a)N_a(0)])\}. \tag{2.47}$$

When the number of C_b elements is constant and the survivability of system H decreases, the necessary number of protective elements clearly increases rapidly. In this case, the greater their effectiveness, the smaller the number of protective elements required for carrying out one and the same task. With an increase in survivability the necessary number of protective elements can be decreased.

Now, let systems H and N have a fixed amount E_a and E_b of a certain substratum (e.g., energy) and be able to distribute it evenly between their protective elements, so that for each fraction of R_a and R_b elements there is $E_{1a} = E_a/N_{Ra}(0)$ and $E_{1b} = E_b/N_{Rb}(0)$, respectively. Then the efficiency coefficients of the protective elements must increase as the E_{1a} and E_{1b} portions increase, since in this case the probabilities of D_a and D_b increase. Therefore, let $D_a = 1 - \exp\{-F_a F_{1a}^{\alpha}\}$, $D_b = 1 - \exp\{-F_b F_{1b}^{\beta}\}$, where F_a, F_b, α, and β are independent of the number of protective elements. This then gives the following expressions for the coefficients of

effectiveness of the protective elements:

$$\left.\begin{aligned} d_a &= -\theta_a \ln(1 - D_a) = -\theta_a F_a E_{1a}^{\alpha} = G_a N_{Ra}^{-\alpha}(0), \\ d_b &= -\theta_b \ln(1 - D_b) = -\theta_b F_b E_{1b}^{\beta} = G_b N_{Rb}^{-\beta}(0), \end{aligned}\right\} \tag{2.48}$$

where $G_a = \theta_a F_a E_a^{\alpha}$, $G_b = \theta_b F_b E_b^{\beta}$. From equations (2.47) and (2.48) we obtain the following transcendental equations for the number of necessary protective elements in systems H and N:

$$N_{Ra}(0) = N_{Ra}^{\alpha}(0) G_a^{-1} \{\ln[G_a M_b(0)/f_1] - \alpha \ln N_{Ra}(0)\}, \tag{2.49}$$

$$N_{Rb}(0) = N_{Rb}^{\beta}(0) G_b^{-1} \{\ln[G_b M_a(0)/f_2] - \beta \ln N_{Rb}(0)\}, \tag{2.50}$$

where

$$f_1 = \ln[eG_a(1 - \theta_a) N_a(0) N_{Ra}^{-\alpha}], \qquad f_2 = \ln[eG_b(1 - \theta_b) N_b(0) N_{Rb}^{-\beta}(0)].$$

Close study of equations (2.49) and (2.50) reveals that in this case the number $N_{Ra}(0)$ is very sensitive with respect to changes in the quantity $\ln[(1 - \theta_a) N_a(0)]$. What is more, this is natural, since with the increase in the number of R_a elements their effectiveness sharply decreases. It is clear that there exists a certain optimal level for the number of protective elements. This level is defined by the assigned survivability of the system. It is better to have a small number of R_a elements of high effectiveness than a large number of R_a elements of low effectiveness. When $k = 3$, from equations (2.37)–(2.39) we have:

$$Q_1 = \sum_{i=1}^{3} m_a(i - 1) \exp[-\alpha N_{Ra}(i - 1)], \tag{2.51}$$

where

$$\left.\begin{aligned} N_{Ra}(1) &= N_{Ra}(0) - m_{Ra}(0) \exp[-d_a N_{Ra}(0)], \\ N_{Ra}(2) &= N_{Ra}(0) - m_{Ra}(0) \exp[-d_a N_{Ra}(0)] - m_{Ra}(1) \exp[-d_a N_{Ra}(1)] \\ &\quad \times m_a(1) + m_a(0) + m_a(2) + m_{Ra}(1) + m_{Ra}(0) + m_{Ra}(2) \\ &= M_b(0). \end{aligned}\right\} \tag{2.52}$$

Equations (2.51) and (2.52) show that the function Q_1 reaches its maximum value when $m_a^*(0) = m_{Ra}^*(2) = m_{Ra}^*(1) = 0$ with this maximum value being independent of the distribution of C_a elements during the last two steps. In this case, $Q_1^*(3) = Q_1^*(2)$. An analogous result is also obtained for system N.

Thus, for an identical game, say system N can for instance destroy at the most $Q_1^*(2) = M_b(0) \exp[-d_a N_{Ra}(0)]$ of a elements; when the number of steps is greater than 2, system N can destroy no more than $Q_1^*(2) = (ed_a)^{-1} \exp[d_a Q_1^*(1)]$ of a elements. Therefore, by comparing $Q_1^*(1)$ with $Q_1^*(2)$ we can see that in the analyzed antagonistic situation the best strategy for both systems is to carry out all allowable operations in two steps. During the first step the action of a portion of each system's C elements is to be set against the protective elements of the opposite system, and during the second step the action of the remaining force is

to be set against the working elements of the opposite system. This conclusion completely agrees with the conclusions reached by Krapivin (1978), which were obtained using different methods.

In the models of the interaction of the two systems that have just been examined, it was assumed that the effectiveness of protective elements does not change with respect to time. However, this assumption in many real situations must be withdrawn. Let us consider a case where both systems can vary the effectiveness of protective elements from step to step, so that at each step the effectiveness is independent of the number of protective elements. Let the effectiveness of R_a and R_b elements be equal to d_{1a} and d_{1b}, respectively, during the first step in the two-step case. Similarly, during the second step the effectiveness acquires values d_{2a} and d_{2b} so that $d_{1a} + d_{2a} = 2d_a, d_{1b} + d_{2b} = 2d_b$; that is, the summed value of the effectiveness does not exceed a constant value. As a result, we obtain the following matrix game:

$$\begin{array}{c} \\ d_{1b} = d_{2b} \\ d_{1b} < d_{2b} \\ d_{1b} > d_{2b} \end{array} \begin{array}{c} \begin{array}{ccc} d_{1a} = d_{2a} & d_{1a} < d_{2a} & d_{1a} > d_{2a} \end{array} \\ \left\| \begin{array}{ccc} Q_{11} & Q_{12} & Q_{13} \\ Q_{21} & Q_{22} & Q_{23} \\ Q_{31} & Q_{32} & Q_{33} \end{array} \right\| \end{array},$$

where

$$\left.\begin{aligned} Q_{11} &= (ed_a)^{-1}\exp\{M_b(0)d_a\exp[-d_aN_{Ra}(0)]\} - (ed_b)^{-1}\exp\{M_a(0)d_b\exp[-d_bN_{Rb}(0)]\}, \\ Q_{22} &= Q_{33} = Q_{23} = Q_{32} = (ed_{2a})^{-1}\exp\{(d_{1a} - d_{2a})N_{Ra}(0) + d_{2a}M_b(0)\exp[-d_{1a}N_{Ra}(0)]\} \\ &\quad - (ed_{2b})^{-1}\exp\{(d_{1b} - d_{2b})N_{Rb}(0) + d_{2b}M_a(0)\exp[-d_{1b}N_{Rb}(0)]\}, \\ Q_{12} &= Q_{\underline{13}} = (ed_{2a})^{-1}\exp\{(d_{1a} - d_{2a})N_{Ra}(0) + d_{2a}M_b(0)\exp[-d_{1a}N_{Ra}(0)]\} \\ &\quad - (ed_b)^{-1}\exp\{M_b(0)d_b\exp[-d_bN_{Rb}(0)]\}, \\ Q_{21} &= Q_{31} = (ed_a)^{-1}\exp\{M_a(0)d_a\exp[-d_aN_{Ra}(0)]\} \\ &\quad - (ed_{2b})^{-1}\exp\{(d_{1b} - d_{2b})N_{Rb}(0) + d_{2b}M_b(0)\exp[-d_{1b}N_{Rb}(0)]\}. \end{aligned}\right\} \quad (2.53)$$

The matrix of this game has a saddle-shaped point under the following conditions $M_a(0) \le N_{Rb}(0)\exp[d_bN_{Rb}(0)]$, $M_b(0) \le N_{Ra}(0)\exp[d_aN_{Ra}(0)]$ and that it takes place in the real system.

Thus, for both systems it is advantageous during the first step to provide protective elements with a small amount of effectiveness and to increase their effectiveness during the second step. This is natural, since it is better to lose a greater number of protective elements during the first step, thus securing a reliable defense of the working elements during the second step of the game.

From equation (2.53) it follows that the losses of a and b elements by systems H and N, respectively, will amount to:

$$\left.\begin{aligned} Q_{1^*} &= \exp\{-1 + (d_{1a} - d_{2a})N_{Ra}(0) + d_{2a}M_b(0)\exp[-d_{1a}N_{Ra}(0)]\}/d_{2a}, \\ Q_{2^*} &= \exp\{-1 + (d_{1b} - d_{2b})N_{Rb}(0) + d_{2b}M_a(0)\exp[-d_{1b}N_{Rb}]\}/d_{2b}. \end{aligned}\right\} \tag{2.54}$$

In order to determine the optimum value of the effectiveness of the R_a and R_b elements for each step of the game, we must find:

$$\min_{(d_{1a},d_{2a})} Q_{1^*}(d_{1a}, d_{2a}) \quad \text{and} \quad \min_{(d_{1b},d_{2b})} Q_{2^*}(d_{1b}, d_{2b}).$$

From equation (2.54) we obtain:

$$\begin{aligned} \frac{\partial Q_{1^*}}{\partial d_{1a}} &= 1 + (2d_a - d_{1a})\{2N_{Ra}(0) - M_b(0)[1 + N_{Ra}(2d_a - d_{1a})] \\ &\quad \times \exp[-d_{1a}N_{Ra}(0)]\} = 0, \end{aligned} \tag{2.55}$$

$$\begin{aligned} \frac{\partial Q_{2^*}}{\partial d_{1b}} &= 1 + (2d_b - d_{1b})\{2N_{Rb}(0) - M_a(0)[1 + N_{Rb}(0)(2d_b - d_{1b})] \\ &\quad \times \exp[-d_{1b}N_{Rb}(0)]\}, \end{aligned} \tag{2.56}$$

From equation (2.55) it is evident that if the equation

$$\{(2d_a - d_{1a})/(d_a - d_{1a})\}\exp[-d_{1a}N_{Ra}(0)] = 0.5N_{Ra}(0)/M_b(0) \tag{2.57}$$

has a real root $0 \le d_{1a}^* \le 2d_a$ then system H, by utilizing this root for its own optimum strategy, can guarantee the average losses of elements not exceeding $Q_1^* = [e(2d_a - d_{1a}^*)]^{-1}$. If equation (2.57) does not have a root in the interval $[0, 2d_a]$, the optimum strategy is then determined either by the root of equation (2.55) or by $d_{1a}^* = 0$. In particular, when $M_b(0) = N_{Ra}(0)$, then $d_{1a}^* = 0$.

Similar calculations are carried out for equation (2.56).

2.4 STABLE STRATEGIES WITHIN THE SURVIVABILITY MODEL

The task of equations (2.11)–(2.13) is solved by means of game theory algorithms. There are many models that simulate the above situations describing the system interaction. Below the two-player antagonistic game is considered.

In game $\Gamma(M, [0, 1])$ with gain function $M(x, y)$ $(0 \le x, y \le 1)$ player I can receive no fewer than

$$v_1 = \max_F \min_G \int_0^1 E_1(F)\, dG(y) = \max_F \min_y E_1[F(y)],$$

where F and G are strategies of the first and second players, respectively:

$$E_1[F] = \int_0^1 M(x, y)\, dF(x).$$

Similarly, player II can receive no more than

$$v_2 = \min_G \max_F \int_0^1 E_2(G)\, dF(x) = \min_G \max_x E_2[G(x)],$$

where

$$E_2[G] = \int_0^1 M(x, y)\, dG(y).$$

Obviously if there exist F^* and G^* such that

$$E_1[F^*] = E_2[G^*] = v_1 = v_2 = v \tag{2.58}$$

then the functions F^* and G^* are the optimal strategies of the players.

Let us consider the game with the gain function:

$$\left.\begin{aligned}
&M(x-y) = \alpha_{k+1} \quad \text{for } x - y \le -\sum_{j=1}^{k} \varepsilon_j, \\
&M(x-y) = \alpha_i \quad \text{for } -\sum_{j=1}^{i} \varepsilon_j < x - y \le -\sum_{j=1}^{i-1} \varepsilon_j \quad (i = \overline{1,k}); \\
&M(x-y) = \beta_j \quad \text{for } \sum_{i=1}^{j-1} \delta_i < x - y \le \sum_{i=1}^{j} \delta_i \quad (j = \overline{1,s}); \\
&M(x-y) = \beta_{s+1} \quad \text{for } x - y > \sum_{i=1}^{s} \delta_i,
\end{aligned}\right\} \tag{2.59}$$

where α_i and β_j are arbitrary real numbers; ε_j and δ_i are positive quantities representing the step lengths of function M; and k and s are natural positive numbers. The number of steps for function M is $k + s + 2$.

Let players I and II choose arbitrary values x and y from $[0, d]$, respectively. The next theorem is valid.

Theorem 2.1 *If equation*

$$\sum_{i=1}^{k} (\alpha_{i+1} - \alpha_i)\lambda^{-\psi_i} + \sum_{j=1}^{s} (\beta_j - \beta_{j+1})\lambda^{\gamma_j} = \beta_1 - \alpha_1 \tag{2.60}$$

where

$$\psi_i = \sum_{j=1}^{i} \delta_j, \qquad \gamma_j = \sum_{i=1}^{j} \delta_i$$

has at least one root $\lambda^* = \rho \exp(i\omega)$ such that $\omega \le \pi/(l + r)$, then stable strategies exist in the game with gain function (2.59) and they are optimal. Under this the

game solution has the form:

$$F^*(x) = (\rho_0)^x[C_1\cos(\omega_0 x) + C_2\sin(\omega_0 x)] + B, \quad -r \le x \le l;$$
$$G^*(y) = D[1 - (\rho_0)^y\cos(\omega_0 y)], \quad 0 \le y \le n;$$
$$v = [\beta_{s+1}(\rho_0)^n - \alpha_{k+1}\cos(\omega_0 n)]/[(\rho_0)^n - \cos(\omega_0 n)],$$

where the root of equation (2.60) $\lambda^* = \rho_0\exp(i\omega_0)$ *has minimal argument and maximal module; r, l, and n are minimal natural numbers that are greater than* ψ_k, $d + \gamma_s$, *and d, respectively:*

$$D = (\beta_0)^n/[(\rho_0)^n - \cos(\omega_0 n)];$$
$$B = \cos(\omega_0 n)[\cos(\omega_0 n) - (\rho_0)^n]^{-1};$$
$$C_1 = [(\rho_0)^{n-1}\sin(\omega_0 r) + (\rho_0)^{n-r}\cos(\omega_0 n)\sin(\omega_0 l)]/\{\sin[(r+l)\omega_0][(\rho_0)^n - \cos(\omega_0 n)]\};$$
$$C_2 = [(\rho_0)^{n-r}\cos(\omega_0 r) - (\rho_0)^l\cos(\omega_0 n)\cos(\omega_0 l)]/\{(\rho_0)^{l-r}\sin[(r+l)\omega_0][(\rho_0)^n - \cos(\omega_0 n)].$$

The proof of the theorem is based on solving equation (2.58) under function (2.59).

Let us now consider the game with gain function $M(x-y)$. In analogy with (2.58), we have:

$$\int_0^1 M(x-y)p_1(x)\,dx = \int_0^1 M(x-y)p_2(y)\,dy = v \tag{2.61}$$

where $dF(x) = p_1(x)\,dx$; and $dG(y) = p_2(y)\,dy$.

Equations (2.61) are solved by means of the Fourier transform:

$$R_2(-p^2)v = R_1(-p^2)p_1(y) \tag{2.62}$$
$$R_2(-p^2)v = R_1(-p^2)p_2(x) \tag{2.63}$$

where $R_1(\omega^2)$ and $R_2(\omega^2)$ are polynomials with real coefficients defined from equations (2.61).

Theorem 2.2 *If the solution* $\bar{p}_1(x) \ge 0$ *of equation (2.62) exists, the game with gain function* $M(x-y)$ *has optimal stable strategies* $p_1^*(x)$ *and* $p_2^*(y)$ *such that*

$$p_1^*(x) = p_2^*(x) = K\bar{p}_1(x) + \sum_{i=1}^{\infty}[A_i\delta^{(i-1)}(x) + B_i\delta^{(i-1)}(x-1)],$$

where $\delta(x)$ *is the delta function; and the constants K,* A_i, *and* B_i *are determined from (2.61) and the conditions:*

$$\int_0^1 p_1^*\,dx = \int_0^1 p_2^*\,dy = 1.$$

Example 2.1. Let us pay attention to the game $\Gamma(M,[0,1])$ with gain function $M(x-y)=a[\delta(x-y)+d\exp\{-b|x-y|\}]$, where a, b, and d are arbitrary constants.

It is easy to see that Theorem 2.2 gives the following solution to this game:

$$p_1(x)=p_2(x)=vb^2(1+A\exp\{\gamma x\}+B\exp\{-\gamma x\})[a\gamma^2]^{-1},$$
$$v=a\gamma^2b^{-2}[1+A(e^{\gamma}-1)/\gamma-B(e^{-\gamma}-1)/\gamma]^{-1},$$

where $\gamma^2=b^2+2db$,

$$A=(\gamma-b)b^{-1}[(\gamma+b)^2-(\gamma^2+b^2)e^{-\gamma}][(\gamma+b)^2e^{\gamma}-(\gamma-b)^2e^{-\gamma}]^{-1},$$
$$B=-(\gamma+b)b^{-1}[(\gamma^2+b^2)e^{\gamma}-(\gamma-b)^2)][(\gamma+b)^2e^{\gamma}-(\gamma-b)^2e^{-\gamma}]^{-1}.$$

Example 2.2. It is easy to find the solution to game $\Gamma(M,[0,1])$ with gain function

$$M(x-y)=\sum_{i=1}^{n}a_i\exp(-b_i|x-y|).$$

From Theorem 2.2 it follows that

$$p_1(x)=p_2(x)=v\left\{a[\delta(x)+\delta(x-1)]+\sum_{j=1}^{n-1}c_j[\exp(-b_jx)+\exp\{-b_j(1-x)\}]+\theta_{2n}/\rho_{2n}\right\}$$
$$v=\left\{2a+\sum_{j=1}^{n-1}2a_j[1-\exp(-b_j)]/b_j+\theta_{2n}/\rho_{2n}\right\}^{-1},$$

where a is an arbitrary root of $R_2(\omega^2)$; and c_j $(j=1,\ldots,n)$ are roots of $R_1(\omega^2)$.

Example 2.3. Let us consider the game with gain function:

$$M(x,y)=\begin{cases}1 & \text{for } (x,y)\in G_1,\\ a & \text{for } (x,y)\in G_a,\\ b & \text{for } (x,y)\in G_b,\end{cases}$$

where $x\in X$, $y\in Y$, $G_1\cup G_a\cup G_b=X*Y$, $G_1=\{(x,y):\rho(x,y)<\varepsilon, x\in K_m\}$, $G_a=\{(x,y):\rho(x,y)\geq\varepsilon\}$, $G_b=\{(x,y):\rho(x,y)<\varepsilon, x\in X\setminus K_m\}$; ε is an arbitrary value; X and Y are m-dimensional bit cubes; K_m is an arbitrary set having volume 0.5; $\rho(x,y)$ is the distance between x and y; and $a=k\varepsilon^m$.

It is obvious that

$$p_1^*(x)=p_2^*(x)=\begin{cases}2/(1+\lambda) & \text{for } x\in K_m,\\ 2\lambda/(1+\lambda) & \text{for } x\in X\setminus K_m,\end{cases}$$
$$v=\varepsilon^m(2\lambda b\pi^{0.5m}\Gamma(m/2)(1+\lambda)^{-1}-kb)+O(\varepsilon^m),$$

where $\lambda=(1-a)/(b-a)$ and $\Gamma(m/2)$ is a gamma function.

2.5 BIOCOMPLEXITY RELATED TO ECOSYSTEM SURVIVAVILITY

The interaction of various elements and processes in the global nature–society system (NSS) has recently attracted the attention of many scientists. Attempts to estimate and predict the dynamics of this interaction have been made in different scientific spheres. One of these attempts is the Biocomplexity Program set up in the U.S.A. by the National Scientific Foundation, within which plans to study and understand relationships between the dynamics of complexity of biological, physical, and social systems and trends in changes of the present habitat. Within the framework of this program, the complexity of the system interacting in some way or another with the environment is connected with phenomena appearing as a result of global-scale contact of a living system with the environment.

Biocomplexity is a derivative of the biological, physical, chemical, social, and behavioral interactions of environmental subsystems, including living organisms and global population. As a matter of fact, the notion of biocomplexity in the environment is closely connected with the rules of biosphere functioning as a combination of its forming ecosystems and natural-economic systems of different scales, from local to global. Therefore, to determine biocomplexity and to estimate it, a combined formalized description is needed of the biological, geochemical, geophysical, and anthropogenic factors and processes taking place at a given level of the spatiotemporal hierarchy of units and scales.

Biocomplexity is a characteristic feature of all systems of the environment connected with life. Elements of this manifestation are studied within the framework of the theory of stability and ecosystem survivability. Note should be taken here that biocomplexity includes indicators of the degree of mutual modification of interacting systems, and this means that biocomplexity should be studied considering both the spatial and biological levels of organization. The difficulty lies in the complicated behavior of the object under study, especially if the human factor is considered, as a result of which the number of stress situations in the environment is constantly growing.

Humankind has accumulated a great deal of knowledge about environmental systems. Use of this knowledge to study biocomplexity is possible within the framework of synthesizing a global model that reflects the laws of interactions between environmental elements and permits assessing just how efficienct it is at constructing different scenarios in the development of human society, based on the actual data of ground and satellite measurements. It it this problem that serves the basis of all questions set forth by the Biocomplexity Program.

Studies of the interaction process are aimed as a rule at understanding and assessing the consequences of a given interaction. The reliability and accuracy of these assessments depend on criteria that serve as the basis for expert examination and recommendations. At present, there is no agreed method to select such criteria for lack of a single scientifically substantiated approach to ecological normalization of economic forcings on the environment. The choice of such criteria determines the accuracy of the ecological expertise made available to

those making decisions about existing and planned human activities and the representativeness of global geoinformation monitoring data.

The processes taking place in the environment can be represented as the totality of interactions between its subsystems. Since a human is one of its elements, it is impossible to definitely divide the environment, for instance, into the biosphere and society: everything on the Earth is correlated and interconnected. The point is to find mechanisms to describe such correlations and interdependences that would reliably reflect the environmental dynamics and answer the questions formulated in the Biocomplexity Program:

1. How does the complexity of biological, physical, and social systems in the environment manifest themselves and change?
2. What mechanisms lie behind the spontaneous development of numerous phenomena in the environment?
3. How do systems of the environment with living components, including those created by humans, react and adjust themselves to stress situations?
4. In what ways do information, energy, and matter move within the systems of the environment and though their levels of organization?
5. Is it possible to predict the system's adaptability and to give prognostic estimates of its changes?
6. How does humankind affect and respond to biocomplexity in natural systems?

One can add many other, no less important questions. For instance, up to what level of complexity should spaceborne observation systems be improved so that their information was of a sufficiently high standard to reliably estimate the state of the environment, if only at the moment of receiving this information? No less important is the question about optimal allocation of the means of geoinformation monitoring at different levels of its organization. Finally, one of the main questions in modern environmental science is estimation of biosphere survivability under conditions of increasing anthropogenic impact. In our opinion such an estimation can be brought about by using the global NSS model and by applying a biocomplexity index. This chapter proposes an approach to resolving this. The general idea is in the combined use of biological complexity and survivability as indicators of the NSS state. Using state-of-the-art simulations, the results presented in this chapter provide an evaluation of the NSS capability to survive under different scenario realizations.

2.5.1 Biocomplexity and survivability indicators

Processes that have their origin in the environment can be presented as the combination of interactions between its subsystems. The human subsystem is a part of the environment and it is impossible to divide the environment into separate subsystems such as biosphere and society. The problem is to search for methodologies to describe existing feedbacks between nature and humanity and to simulate dynamic tendencies in the NSS reliably. Unfortunately, the part of the

NSS that is responsible for the quality of modeling climatic processes introduces instability in the modeling results. This is the reason that we suppose below that the NSS climatic component can be replaced by a scenario describing stable climatic trends during the time interval of investigation. What is actually studied is the NSS.

Let us introduce the scale symbol Ξ of biocomplexity ranging from the state where all interactions between environmental subsystems are broken to the state where they correspond to natural evolution. In this case, we have an integrated indicator of the environmental state including bioavailability, biodiversity, and survivability. It reflects the level of all types of interactions among environmental subsystems. In reality, specific conditions exist where these interactions are changed and transformed. For example, under the biological interaction of consumer/producer type or competition-for-energy-resource type there exists some minimal level of food concentration where contacts between interacting components cease. Physical, chemical, and other types of interactions in the environment commonly depend on specific critical parameters. Environmental dynamics is regulated by these parameters and the main task is its parametrical description. Biocomplexity reflects these dynamics.

All of this corroborates the fact that biocomplexity is related to categories that are difficult to measure empirically and to express quantitatively. However, we will try to transfer truly verbal tautological reasoning to formalized quantitative definitions. For the transition to gradations of the scale Ξ with quantitative positions it is necessary to postulate that relationships between two values of Ξ are of the type $\Xi_1 < \Xi_2$, $\Xi_1 > \Xi_2$, or $\Xi_1 \equiv \Xi_2$. In other words, there always exists a value of the scale ρ that defines a biocomplexity level $\Xi \to \rho = f(\Xi)$, where f is a certain transformation of the biocomplexity concept to a number. Let us attempt to search for a satisfactory model to simulate the verbal biocomplexity image in constructive terms, subordinating it to formal description and transformation. With this purpose in mind m subsystems of the NSS are selected. The correlations between these subsystems are defined by the binary matrix function $X = \|x_{ij}\|$, where $x_{ij} = 0$, if subsystems B_i and B_j do not interact, and $x_{ij} = 1$, if subsystems B_i and B_j are interacting. Then, any one point $\xi \in \Xi$ is defined as the sum $\xi = \sum_{i=1}^{m} \sum_{j>i}^{m} x_{ij}$. Of course, there arises the need to overcome uncertainty for which it is necessary to complicate the scale Ξ (e.g., by introducing weight coefficients for all NSS subsystems). The origin of these coefficients depends on the type of subsystem. This is the reason three basic subsystem types are selected: living, nonliving, and vegetation. Living subsystems are characterized by their density, determined by the number of their elements or by biomass value per unit area or volume. Vegetation is characterized by the type and portion of occupied territory. Nonliving subsystems are measured by their concentration per unit area or volume of the environment. In the common case, certain characteristics $\{k_i\}$, corresponding to the significance of subsystems $\{B_i\}$, are assigned to every subsystem B_i $(i = 1, \ldots, m)$. As a result we obtain a better definition of the formula to move

from the biocomplexity concept to the scale Ξ of its indicator:

$$\xi = \sum_{i=1}^{m} \sum_{j>i}^{m} k_j x_{ij}. \tag{2.64}$$

It is clear that $\xi = \xi(\varphi, \lambda, t)$, where φ and λ are the geographical latitude and longitude, respectively, and t is the current time. For the territory Ω the biocomplexity indicator is defined as the mean value:

$$\xi_\Omega(t) = (1/\sigma) \int_{(\varphi,\lambda) \in \Omega} \xi(\varphi, \lambda, t)\, d\varphi\, d\lambda$$

where σ is the area of Ω.

Thus, the indicator $\xi_\Omega(t)$ is the characteristic of integrated NSS complexity that reflects the individuality of its structure and behavior at each time t in space Ω. According to the laws of natural evolution a decrease (increase) in $\xi_\Omega(t)$ will correspond to an increase (decrease) of biocomplexity and the survivability of the nature–anthropogenic systems. Since a decrease in biocomplexity disturbs biogeochemical cycles and leads to a decrease in stress on the nonrenewal of resources, then the binary structure of the matrix X changes direction to intensify resource impoverishment technologies. The vector of energy exchange between NSS subsystems is moved to a position where the survivability level of the NSS is reduced.

The global simulation model is constructed with the spatial resolution of the Earth's surface in which $\Delta\varphi$ represents latitude and $\Delta\lambda$ longitude. In other words, the NSS space Ω is divided into a set of pixels Ω_{ij} ($\Omega = \bigcup \Omega_{ij}$; $\Omega_{ij} = \{((\varphi, \lambda); \varphi_i \le \varphi < \varphi_{i+1}; \quad \lambda_j \le \lambda < \lambda_{j+1}; \quad i = 1, \ldots, N; \quad j = 1, \ldots, M; \quad N = [180/\Delta\varphi]; M = [360/\Delta\lambda]\}$). Each cell Ω_{ij} has its own biocomplexity indicator value:

$$\xi_\Omega(i,j,t) = (1/\sigma_{ij}) \int_{(\varphi,\lambda) \in \Omega_{ij}} \xi(\varphi, \lambda, t)\, d\varphi\, d\lambda. \tag{2.65}$$

The value $\xi_\Omega(i,j,t)$ calculated by formula (2.65) reflects the topological structure of the matrix $X(i,j,t)$. Consequently, there exist $n = N \cdot M$ matrixes and biocomplexity indicators to characterize NSS biocomplexity. As part of the computer experiment there arises a set of numerical characteristics of NSS biocomplexity distributed in space and time. Integrated NSS biocomplexity indicators can be calculated for any arbitrary area $\omega \in \Omega$:

$$\xi_\omega(t) = (1/\sigma_\omega) \sum_{(\varphi_i,\lambda_j) \in \omega} \xi_\Omega(i,j,t). \tag{2.66}$$

This can be average NSS biocomplexity by longitude or latitude zone, by ocean or sea aquatory, by country or state territory, etc.

NSS survivability is closely connected with biocomplexity. In the common case the behavior of any system is determined by the values characterizing the state of the system, which can take different terms. Upon interaction with an external medium and, in particular, with other systems, the values of these terms can vary in one way or another. For any technological or biological system, it is

always possible to show the field of change of the characteristic parameters, wherein the system can be considered to be functioning. Outside this field the system does not exist. Thus, one can substitute the complex behavior of a system by depicting this system as a point in the phase space of the characteristic parameters. If the change of any coordinate leads to the disappearance of the depicting point from the allowable field, the system collapses (the organism as a whole perishes).

Let us restate what we said in the introduction to this chapter (Section 2.1) about significant variables not being identical regarding the degree of threat they pose to the system. Such variables as the oxygen content of blood or the structural integrity of the medulla oblongata cannot tolerate any significant changes, since such changes would almost invariably lead to immediate death. However, there are changes, such as in the temperature of individual areas of the skin where sharp fluctuations do not necessarily lead to such an eventuality. Separating all variables characterizing the state of the system into significant variables makes it possible to simplify the behavioral strategy of a system as it interacts with an external environment or other systems. A most constructive approach to describing the global environment was proposed by Gorshkov *et al.* (2000). They consider that a different path of development compatible with long-term environmental safety lies through conservation and restoration of a substantial part of the Earth's biosphere to its natural nonperturbed state, bearing in mind the stabilizing potential of the natural biota of Earth with respect to the global environment. The problem of biosphere survivability really does correlate with the mechanisms of biotic regulation, physical and biological stability, the sensitivity of biota, ecological limitations, and other basic principles of biology. In general, each living organism clearly plays a role in global change. The problem lies in describing this role to estimate the significance of interactions between the hierarchy of biospheric elements having various spatial scales and different influences on the levels of biological organization.

Following Krapivin (1978, 1996) a survivability indicator can be taken from trophic relations between ecosystem components and represented by the equation:

$$\nu(t) = \frac{\sum_{i=1}^{m} \int\int_{(\varphi,\lambda)\in\Omega} \int_0^{z_0} B_i(\varphi,\lambda,z,t)\, d\varphi\, d\lambda\, dz}{\sum_{i=1}^{m} \int\int_{(\varphi,\lambda)\in\Omega} \int_0^{z_0} B_i(\varphi,\lambda,z,t_0)\, d\varphi\, d\lambda\, dz},$$

where B_i is the ith element of the NSS.

Indicators such as these and others help to determine the state of an environmental subsystem based on restricted information. Remote sensing of the environment is characterized by a series of such indicators as NDVI, LAI, and SIL, which are used widely in many studies. Of the important problems that are the subject of many international environmental programs the study of forest ecosystems is arguably the most pressing.

Anthropogenic and natural biomass burning has become an ordinary event in the world. The development of an effective technology for atmosphere pollution control by means of satellite system is long overdue. However, there exist difficulties connected with spatial resolution, the temporal frequency of satellite overpasses, and cloudiness. The temporal dynamics of fire cannot be correlated with the interval between two consequent satellite overpasses over the area that is ablaze. Boschetti *et al*. (2003) proposed a methodology of using data acquired by the European Meteosat and the Japanese GMS to detect burned areas in different tropical environments. The methodology is based on a multiple threshold approach applied to thermal radiance and to a spectral index specific to burned surfaces.

Of the informational indexes available, the Simple Index for Burned Areas (SIBA) is the best for adaptation to observational conditions. It allows various features of the burned area to be enhanced:

- low albedo;
- high temperature;
- temperature higher than the surrounding pixels in a window large enough to encompass the burned areas.

SIBA can be described as a normalized function:

$$\mathrm{SIBA}_{ij} = I_{ij}/(I_{ij} + 1),$$

where

$$I_{ij} = \left[\frac{(T_{ij} - a)(T_{ij} - b)}{c\rho_{\mathrm{TOA}_{ij}}(\hat{T}_{ij} - b)}\right]^2;$$

T_{ij} is the surface temperature (K) of pixel Ω_{ij}; $\hat{T}_{ij}$ is the mean surface temperature (K) in a window of 60×60 pixels around pixel Ω_{ij}; $a = 248$, $b = 273$, $c = 300$; and $\rho_{\mathrm{TOA}_{ij}}$ is the top-of-atmosphere reflectance of pixel Ω_{ij}.

Numerous calculations made by Boschetti *et al*. (2003) show that SIBA behaves differently in some significant cases: water bodies, clouds, and burnt surfaces. SIBA maintains the capability to detect burned areas in different areas and under different conditions. This capability depends on the sensor type.

The introduction of integral characteristics for use as indicators of the state of the environmental subsystem (as demonstrated by many authors) allows satellite monitoring of soil–plant formations. The most appropriate index here is the Scattering Index over Land (SIL), which permits different surfaces to be distinguished:

$$\mathrm{SIL} = 451.9 - 0.44T_b(19\,\mathrm{GHz}) - 1.755T_b(22\,\mathrm{GHz}) + 0.00575T_b^2(22\,\mathrm{GHz}) - T_b(85\,\mathrm{GHz});$$

$$\mathrm{SIL} = \begin{cases} 10\,\mathrm{K} & \text{precipitation area;} \\ 13\,\mathrm{K} & \text{snow cover;} \\ 15\,\mathrm{K} & \text{desert or semidesert territory.} \end{cases}$$

SIL facilitates solution of a precipitation problem:

$$RR(\text{mm/h}) = 0.00513 \cdot \text{SIL}^{1.9468}.$$

There exist other correlations as functions of integral indexes. For example, low atmospheric temperature can be estimated by means of the following formula:

$$T(\text{K}) = 58.08 - 0.39T_{bv}(19\,\text{GHz}) + 1.21T_{bv}(22\,\text{GHz}) - 0.37T_{bv}(37\,\text{GHz}) + 0.36T_{bv}(85\,\text{GHz}).$$

According to this, when $T > T^*$ precipitation is possible, where

$$T^* = \begin{cases} 242.5 + 5\cos\theta & \text{for } T_b(53.6\,\text{GHz}) \le 248\,\text{K}; \\ 0.667[T_b(53.6\,\text{GHz}) - 248] + 252 + 6\cos\theta & \text{for } T_b(53.6\,\text{GHz}) > 248\,\text{K}; \end{cases}$$

where θ is the satellite zenith angle.

The NDVI and LAI indexes help to assess the water content of vegetation (kilograms per square meter):

$$m_\nu = \begin{cases} 1.9134(\text{NDVI})^2 - 0.3215(\text{NDVI}) & \text{when NDVI} \le 0.5; \\ 4.2857(\text{NDVI})^2 - 1.5429 & \text{when NDVI} > 0.5. \end{cases}$$

All these correlations help to form (as part of the GIMS) an effective algorithm to assess forest conditions that may be susceptible to fire. Maki *et al.* (2004) proposed the following procedure to predict fire outbreak and propagation. The prediction of fire outbreak, propagation, and scale in forested areas depends mainly on wind direction, vegetation water status, topography, but other factors are involved. Vegetation water status is the most important parameter determining the risk of fire. Maki *et al.* (2004) calculated the vegetation water status at ground level by means of three definitions:

(i) fuel moisture content (FMC);
(ii) equivalent water thickness (EWT);
(iii) relative water content (RWC).

FMC is defined as the ratio between the quantity of water in vegetation and either the fresh or dry weight of vegetation:

$$\text{FMC} = \frac{\text{FW} - \text{DW}}{\text{FW (or DW)}} \times 100(\%).$$

EWT is the ratio between the quantity of water and the area σ:

$$\text{EWT} = \frac{\text{FW} - \text{DW}}{\sigma}(\text{g/cm}^2).$$

RWC is calculated by means of the following formula:

$$\text{RWC} = \frac{\text{FW} - \text{DW}}{\text{TW} - \text{DW}},$$

where FW is the full weight; DW is the dry weight; and TW is the turgid weight.

2.5.2 The nature–society system biocomplexity model

The NSS consists of subsystems B_i $(i = 1, \ldots, m)$ whose interactions are built up over time as a result of the functions of many factors. NSS biocomplexity indicates the structural and dynamic complexity of its components. In other words, NSS biocomplexity is formed under the interaction of its subsystems $\{B_i\}$. Over the course of time, subsystems B_i can change their state and, consequently, change the topology of the relations between them. The evolutionary mechanism of adaptation of subsystem B_i to the environment allows the hypothesis that each subsystem B_i, independent of its type, has structure $B_{i,S}$, behavior $B_{i,B}$, and goal $B_{i,G}$ such that $B_i = \{B_{i,S}, B_{i,B}, B_{i,G}\}$. The strivings of subsystem B_i to achieve certain preferable conditions are represented by its goal $B_{i,G}$. The expedience of structure $B_{i,S}$ and the purposefulness of behavior $B_{i,B}$ for subsystem B_i are estimated by the effectiveness with which goal $B_{i,G}$ is achieved.

As an example, let us consider the process of fish migration. The investigations of many authors have revealed that this process is accompanied by purposeful behavior. From these investigations it follows that fish migrations are subordinated to the principle of complex maximization of effective nutritive rations, subject to favorable environmental conditions (temperature, salinity, dissolved oxygen, pollution level, depth). In other words, the travel of migrating species takes place at characteristic velocities toward the maximum gradient of effective food, subject to ecological restrictions. This is the reason we can formulate that goal $B_{i,G}$ of the fish subsystem is toward increasing its food supply and that behavior $B_{i,B}$ consists in finding the optimum route to attain goal $B_{i,G}$.

Since the interactions of subsystems B_i $(i = 1, \ldots, m)$ are connected with chemical and energy cycles, it is natural to suppose that each subsystem B_i accomplishes the geochemical and geophysical transformation of matter and energy to remain in a stable state. The formal approach to this process consists in supposing that interactions between NSS subsystems are represented as a process whereby the systems exchange a certain quantity V of resources spent in exchange for a certain quantity W of resources consumed. We shall call this process "(V, W) exchange".

The goal of subsystem B_i is the most advantageous (V, W) exchange (i.e., it tries to get maximum W in exchange for minimum V). The quantity W is a complex function of the structure and behavior of interacting subsystems, $W = W(V, B_i, \{B_k, k \in K\})$, where K is the set of subsystem numbers interacting with subsystem B_i.

Let us designate $B_K = \{B_k, k \in K\}$. Then, the following (V, W) exchange is the result of interactions between subsystem B_i and its environment B_K:

$$W_{i,0} = \max_{B_i} \min_{B_K} W_i(V_i, B_i, B_K) = W_i(V_i, B_{i,\text{opt}}, B_{K,\text{opt}})$$

$$W_{K,0} = \max_{B_K} \min_{B_i} W_K(V_K, B_i, B_K) = W_K(V_K, B_{i,\text{opt}}, B_{K,\text{opt}}).$$

Hence, it follows that some range of the goal of subsystem B_i exists which defines the levels of V_i and V_K. Since limiting factors are defined by nature, then

it is natural to suppose in this case that some level $V_{i,\min}$ exists when subsystem B_i ceases to spend its energy resources on external resources (i.e., if $V_i \leq V_{i,\min}$, subsystem B_i concentrates on regenerating its internal resources). In other words, when $V_i \leq V_{i,\min}$, any decrease in the biocomplexity indicator $\xi_\Omega(t)$ takes place at the expense of breaking off interactions between subsystem B_i and other subsystems. Commonly, the structure of $V_{i,\min}$ is checkered (i.e., the changeover of x_{ij} from state $x_{ij} = 1$ to state $x_{ij} = 0$ is not realized for all j at the same time). Actually, in any trophic pyramid of living subsystems producer/consumer-type relationships cease when the consumer biomass concentration falls below some critical level. In other cases the interactions between subsystems $\{B_i\}$ can be stopped at the expense of various combinations of its parameters. The parametrical description of possible situations of interactions between subsystems $\{B_i\}$ can be realized in the NSS simulation model.

2.5.3 Simulation experiments

2.5.3.1 The Okhotsk Sea ecosystem case

The Okhotsk Sea ecosystem (OSE) is a significant element of the biosphere whose evaluation requires development of a common criterion. The OSE Biocomplexity Index helps to explain many processes regulating the interactions between biotic components, hydrodynamic effects, and energy fluxes. Traditional estimates of the contributions from different processes within the OSE deal with the study of local or special parameters. This makes understanding correlations between OSE components and forecasting their dynamics impossible. Moreover, a simple index would make it possible to evaluate the state of the OSE by means of ordinary calculations.

The OSE has a trophic graph showing interactions at many levels between biological, chemical, and physical processes. OSE biocomplexity consists of numerous sets of biotic regulations determining the fundamental properties of living objects. An important property of OSE living components is that all biological species exist in the form of populations. All processes and phenomena observed in the OSE are characterized by a certain degree of physical and biological stability, which is a function of external and internal fluxes of energy. External fluxes of energy are defined as solar irradiation, the influence of the Pacific Ocean, and anthropogenic interventions. In the absence of an external flux of energy, the OSE tends toward a state of thermodynamic equilibrium, which is characterized by the maximum degree of chaos possible in a given system (Gorshkov *et al.* 2000).

In any event, OSE dynamics is a complex function of many parameters having different chemical, physical, and biological character. A biocomplexity index has to reflect this and to characterize the biological stability of the whole aquageoecosystem.

The Okhotsk Sea is a typical highly productive sea whose ecosystem has to function under severe climatic conditions. The spatiotemporal structure of the

basic hydrological and ecological characteristics of the Okhotsk Sea is heterogeneous. The chemical, physical, and biological processes occurring in seawater have been studied by many authors to assess their bioproductivity. According to the investigations made by Terziev *et al.* (1993), the following structural discretization of the Okhotsk Sea geoecosystem can be realized. Five ecological layers exist. Layer 1 is where photosynthesis is greatest. It is situated above the thermocline and lies at depths of 20–30 m. It corresponds to the wind-mixed layer. Layer 2 occupies depths from 30 to 150 m. It has a low temperature and oxygen saturation of about 80–90%. Layer 3 is characterized by low oxygen saturation (15–20%). It lies at depths of 150–750 m. Layer 4 extends from 750 m down to a depth of 1,500 m. This layer has the lowest oxygen saturation (10–15%). Lastly, layer 5 is located deeper than 1,500 m. It is characterized by oxygen saturation of 25–30%.

The Okhotsk Sea aquatory is divided into zones having specific ecological features (Suzuki, 1992). The spatial distribution of fish depends on seasonal conditions and to a great extent correlates with the layers just mentioned. The use of the sea's biological resources is a function of this distribution. Fishing intensity essentially depends on knowledge of the biomass distribution in zones that have their own specific environmental conditions. Various authors (Aota *et al.*, 1992; Nitu *et al.*, 2000b; Plotnikov, 1996) have tried to resolve this by using models that simulate ecosystem dynamics. However, the modeling results have not always turned out to be sufficiently representative and to reflect the classification of sea zones according to their productivity. The biocomplexity indicator is one such simple form capable of identifying these zones. It has been shown by many investigators that highly productive Okhotsk Sea zones are characterized by a complex multilevel trophic graph (Terziev *et al.* 1993). However, this effect is not universal. For instance, the ecosystem of the Peruvian Current is highly productive in zones where the trophic graph is short (Krapivin, 1996). These situations can be distinguished by migration processes. Hence, the biocomplexity of ecosystems can be formed in various ways.

Let us consider the following components of the Okhotsk Sea ecosystem (Table 2.1). The trophic pyramid $X = \|x_{ij}\|$, where x_{ij} is a binary value equal to "1" or "0" under the existence or absence of nutritive correlations between the ith and jth components, respectively. Let us define the biocomplexity function as:

$$\xi(\varphi, \lambda, z, t) = \sum_{i=1}^{20} \sum_{j=1}^{19} x_{ij} C_{ij}, \tag{2.67}$$

where φ and λ are the geographical latitude and longitude; t is current time; z is depth; $x_{ij} = 1$ if $B_m \geq B_{m,\min}$ and 0 if $B_m < B_{m,\min}$ where $B_{m,\min}$ is the minimal biomass of the mth component consumed by other trophic levels; $C_{ij} = k_{ji} B_{i,*} / \sum_{j,+}$ is the nutritive pressure placed by the jth component on the ith component; $\sum_{i,+} = \sum_{m \in S_i} k_{im} B_m$ is the real store of food available to the ith component; $B_{m,*} = \max\{0, B_m - B_{m,\min}\}$; $k_{im} = k_{im}(t, T_W, S_W)$ $(i = 1, \ldots, 17)$ is the satisfaction index of the nutrition requirements of the ith component at the expense of the biomass of the mth component; k_{im} $(i = 18, 19)$ is the trans-

Table 2.1. Trophic pyramid of the Okhotsk Sea ecosystem considered when calculating the biocomplexity indicator. Notation: B_{14} *Reinhardti ushippoglossoi des matsuurae*; B_{15} *Clupeapallasi pallasi* Val.

Consumers of energy and matter	*Sources of energy and matter*																		
	B_1	B_2	B_3	B_4	B_5	B_6	B_7	B_8	B_9	B_{10}	B_{11}	B_{12}	B_{13}	B_{14}	B_{15}	B_{16}	B_{17}	B_{18}	B_{19}
Phytoplankton, B_1	0	0	0	0	0	0	0	0	0	0	0	0	0	0	0	0	0	1	0
Bacterioplankton, B_2	0	0	0	0	0	0	0	0	0	0	0	0	0	0	0	0	0	0	1
Microzoa, B_3	1	1	0	0	0	0	0	0	0	0	0	0	0	0	0	0	0	0	1
Microzoa, B_4	1	1	0	0	0	0	0	0	0	0	0	0	0	0	0	0	0	0	0
Carnivores, B_5	0	1	1	1	1	0	0	0	0	0	0	0	0	0	0	0	0	0	1
Zoobenthic animals, B_6	1	1	1	1	1	0	0	0	0	0	0	0	0	0	0	0	0	0	1
Flat-fish, B_7	0	0	0	0	0	1	1	1	1	1	1	1	1	1	1	1	1	0	0
Coffidae, B_8	0	0	0	0	1	1	1	1	1	1	1	1	1	1	1	1	1	0	0
Ammodytes hexapterus, B_9	0	0	0	0	0	1	1	0	0	1	1	1	0	0	0	1	0	0	0
Mallotus, B_{10}	0	0	0	0	1	1	1	0	0	0	1	0	0	0	0	0	0	0	0
Theragra chalcogramma, B_{11}	0	0	0	0	1	0	0	0	0	1	1	1	0	0	0	0	0	0	0
Salmonidae, B_{12}	0	0	0	0	0	1	1	0	0	1	1	1	1	0	0	1	0	0	0
Coryphaenoides, B_{13}	0	0	0	0	1	1	1	1	1	1	1	1	1	1	1	1	1	0	0
B_{14}	0	0	0	0	1	1	1	1	1	1	1	1	1	1	1	1	1	0	0
B_{15}	0	0	0	0	1	1	0	0	0	0	0	0	0	0	0	0	0	0	0
Crabs, B_{16}	0	0	0	0	0	1	0	1	1	1	0	1	0	0	0	1	1	0	0
Laemonema longipes, B_{17}	0	0	0	0	1	1	0	0	0	0	0	0	0	0	0	0	1	0	0
Biogenic salts, B_{18}	0	0	0	0	0	0	0	0	0	0	0	0	0	0	0	0	0	0	1
Detritus, B_{19}	1	1	1	1	1	1	1	1	1	1	1	1	1	1	1	1	1	0	0
People, B_{20}	1	1	1	1	1	1	1	1	1	1	1	1	1	1	1	1	1	1	1

formation coefficient from the mth component to the ith component; $k_{i,20}$ represents anthropogenic influence on the ith component; $S_i = \{i : x_{ij} = 1, j = 1, \ldots, 19\}$ is the food spectrum of the ith component; T_W is water temperature; and S_W is water salinity.

Let us designate the aquatory of the Okhotsk Sea by $\Omega = \{(\varphi, \lambda)\}$. The value of the biocomplexity indicator for any area $\omega \in \Omega$ is determined by the formula:

$$\xi_\omega(z_1, z_2, t) = (1/\sigma_\omega) \int_{(\varphi,\lambda) \in \omega z_1} \int_{z_1}^{z_2} \xi(\varphi, \lambda, z, t)\, d\varphi\, dz,$$

where $[z_1, z_2]$ is the water layer located between the depths of z_1 and z_2.

The maximum value of $\xi = \xi_{\max}$ (≈ 20) is reached during the spring–summer when nutrition relationships in the OSE are extended, the intensity of energy exchanges is increased, and horizontal and vertical migration processes are stimulated. In winter the value of ξ approaches $\xi_{\min}$ (≈ 8). The spatial distribution of ξ reflects the local variability of the food spectrum for the various components. Figure 2.3 and Table 2.2 show examples of such a distribution. Comparison of this distribution with that of zones with industrial fish accumulations (Terziev *et al.*, 1993) shows that there is a correlation between these distributions.

The indicator ξ reflects the level of complexity of the OSE. A change in ξ is a consequence of migration processes and the variability of nutritive interactions. In

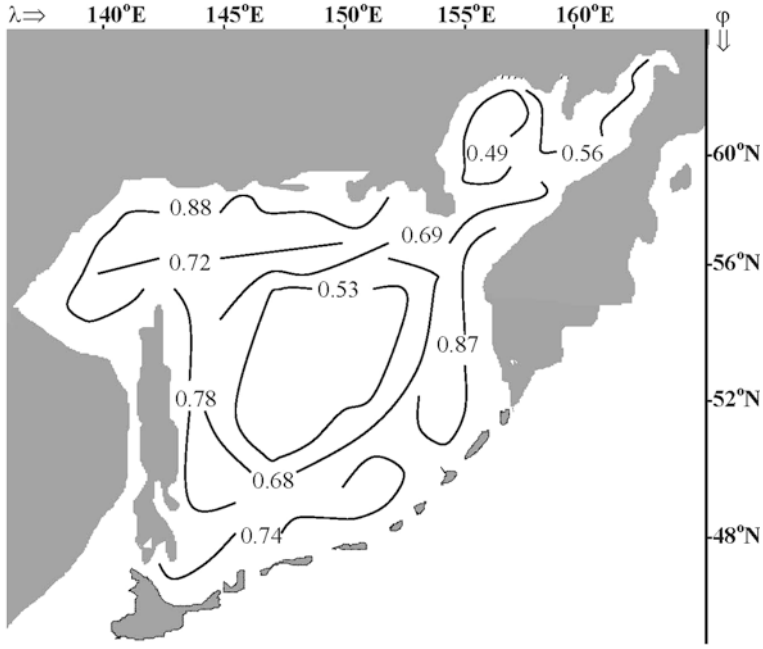

Figure 2.3. Spatial distribution of the biocomplexity indicator $\xi^* = \xi/\xi_{\max}$ for the spring–summer.

Table 2.2. Estimates of the biocomplexity indicator ξ^* for different layers in spring–summer and in winter.

Season	*Layer*				
	1	*2*	*3*	*4*	*5*
Spring–summer	0.89	0.93	0.62	0.34	0.21
Winter	0.31	0.49	0.71	0.39	0.22

these processes subsystem B_{20} plays the role of an external source of change in other components. These changes are interpreted in terms of fishing and impacts causing variations in component biomass.

Calculations show that basic variability in $\xi^* = \xi/\xi_{\max}$ is caused by migration processes. Under these conditions, there occurs a quick redistribution of the interior structure of matrixes X and $\|C_{ij}\|$. For instance, according to Terziev *et al.* (1993) many fish during spring migrate to the shelf zone and during winter they move to the central aquatories of the sea. Therefore, the value of $\xi^* \to 1$ during spring and $\xi^* \to 0.6$ during winter for the shelf zone. This means that the biocomplexity of the Okhotsk sea ecosystem in the shelf decreases by 40% in winter in comparison with spring. For the central aquatories the value of ξ^* varies near 0.7 throughout the year. Such stability of the biocomplexity indicator is explained by the balance between nutrition correlations and productivity during spring, summer, and winter.

It has been established that variability in ξ^* stimulates changes in fish concentrations that are controlled by environmental conditions. Specifically, during spring time the larval Pacific hering (*Clupea pallasi*) occupies the area with $T_W < 5^\circ$C. Other fish have an elective depth for feeding and spawning (Terziev *et al.*, 1993). All these processes influence the variability of ξ^*. More detailed investigation of correlations between the value of ξ^* and the structural and behavioral dynamics of the Okhotsk Sea ecosystem requires additional studies.

This section has introduced a means of moving from a verbal description of biocomplexity to a numerical scale. In future studies it will be necessary to take into consideration various factors such as bottom relief, climate trends, ice field dynamics, detailed components of the trophic pyramid, bottom sediments, and current structure. Moreover, it is necessary to add members describing anthropogenic impacts on the ecosystem considered socioeconomically to formula (2.67).

2.5.3.2 Upwelling ecosystem case

It is known that upwelling zones characterized by vertical water motions have high productivity. An upwelling zone is the result of many phenomena: water removal from the coastline by the wind, changes in ocean currents, etc. Water velocity and

the stability of an upwelling zone are determined by a set of synoptic parameters. The most specific value for the vertical speed of water in an upwelling zone is $0.77 \cdot 10^{-3}\ \mathrm{cm} \cdot \mathrm{s}^{-1}$. The depths at which water flows start vary within 200 m.

Let us proceed from the concept of successive development of a community from the time of its origin in a region invaded by deep water until its climax in the oligotrophic convergence region. In between these times the system develops and moves along with the water flow. In addition, the total energy of the system and its structure (spatial, trophic, and specific) are changed. The observed general characteristics of these changes occurring in time and space are now available, and one of the major criteria determining the adequacy of the model is its agreement with the actual picture observed in the oceans.

Let us suppose ecosystem motion from the upwelling zone is homogeneous in the horizontal plane. The ecosystem state is characterized by depth z with step Δz ($\approx$10 m) and by time t with interval Δt (daily). The horizontal speed of the water current from the upwelling zone is $V = V_\varphi = V_\lambda$, so that the distance of the water volume from the upwelling zone equals $\Delta r = (\Delta\varphi^2 + \Delta\lambda^2) = V \cdot \Delta t$.

The ecosystem state at each layer $z = \mathrm{const}$ is determined by light intensity $E(z,t)$, by nutrient salt concentration $n(z,t)$, and by the biomass of detritus $d(z,t)$, phytoplankton $p(z,t)$, bacterioplankton $b(z,t)$, protozoa $Z_1(z,t)$, microzoa $Z_2(z,t)$, small-sized herbivores $Z_3(z,t)$, large-sized herbivores $Z_4(z,t)$, small predators like *Cyclopodia* $Z_5(z,t)$, intermediate predators like *Calanoida* $Z_6(z,t)$, and large predators like *Chaetognatha* and *Polychaeta* $Z_7(z,t)$. The protozoa include infuzorii and radiolarii. The microzoa include the nauplii stages of copepods. Based on plankton-feeding studies made by many authors (Vinogradov *et al.*, 1972) the small-sized herbivores are now believed to include, apart from the protozoa and nauplii, young copepod stages of *Calanoida* and adult copepods whose size does not reach 1.0 mm such as *Clausocalanus*, *Acrocalanus*, *Paracalanus*, *Calocalanus*, etc. The group of large-sized herbivores consists of animals whose size exceeds 1.0 mm such as *Undinula*, *Eucalanus*, *Rhincalanus*, *Neocalanus*, *Lucicutia*, juveniles of *Euphausiacea*, etc. The group of omnivores includes *Centropages*, *Pleuromamma*, *Scolecithrix*, *Undeuchaeta*, *Conchoecia*, etc., while *Chaetognatha*, *Candacia*, *Euchaeta*, *Cyclopodia*, etc. are grouped with the carnivores.

It is accepted that 30% of the bacterioplankton biomass is held in natural clots of size greater than 3–5 μm, which can be consumed by the herbivores (Z_3 and Z_4). The microzoa (Z_2), protozoa (Z_1), and small-sized herbivores (Z_3) can consume unclotted bacterioplankton as well.

The trophic relations between the components are described by means of the energetic principle (Figure 2.4). Biomass, production, respiration, mortality, and rations are measured by the energy scale in calories per cubic meter or calories per square meter.

When estimating changes in the system over time, it was assumed that water takes more than 60 days to cover the distance from the upwelling zone to the oligotrophic zone of planetary convergence. Figure 2.5 gives a representation of the changes in biomasses as functions of time. We see that the phytoplankton

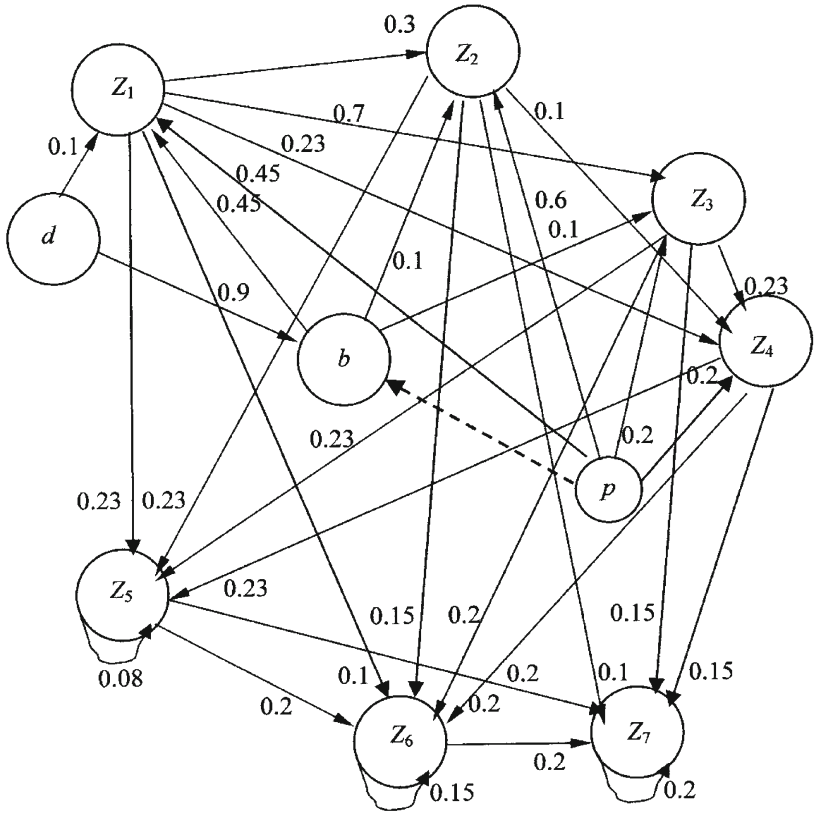

Figure 2.4. Scheme of the trophic interactions between components of the upwelling ecosystem. The values of coefficients C_{ij} are shown on the arrows' shafts.

biomass increases most rapidly here, reaching its maximum ($\approx 4{,}500\,\mathrm{cal}\cdot\mathrm{m}^{-2}$) on the 5th to 10th day of the existence of the system. After this, the phytoplankton biomass decreases. The peak bacterioplankton biomass is reached on the 10th to 15th day. Small-sized herbivores lag somewhat behind phytoplankton in development, and their biomass reaches its peak only on the 30th day. Nevertheless, its influence along with that of nutrient salt decrease leads to a sharp drop in phytoplankton and bacterioplankton biomasses. Namely, inverse chains of the community give weak contributions to R_p and R_b. After the 40th day, the phytoplankton biomass mainly functions at the expense of biogenic elements arriving in the eutrophic zone across the thermocline from deeper layers. Subsequently, the phytoplankton biomass decreases relatively slowly. This is the time that stability factors begin to influence the community at the expense of exterior energy flows.

The carnivores prove to be even more inertial than the herbivores as their biomass attains its peak only on the 35th to 50th day. This is the time (i.e., the 50th to 60th day) that the system reaches its quasistationary state characterized by low concentrations of all living components.

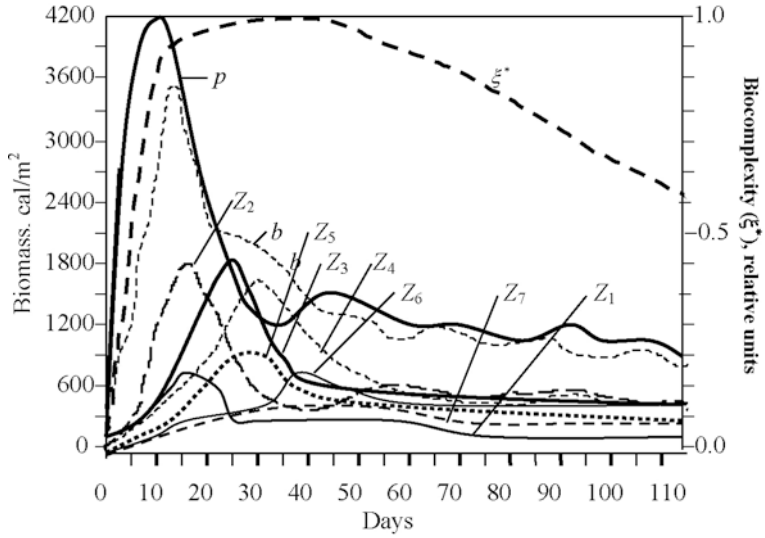

Figure 2.5. Time dependence of the total biomasses of living components of the upwelling ecosystem in the 0–200 m water layer.

2.6 COMPUTER SIMULATION OF ACID RAIN

Key to understanding the state of today's global ecodynamics and ecosystem survivability is the study of conditions for acid rain formation and their prediction. For the first time, this problem was widely discussed at the 28th General Assembly of the International Unit on Theoretical and Applied Chemistry held in Madrid in September 1975. Subsequent conferences and various international programs have made it possible to accumulate data and knowledge in this sphere. Consequently, we now know that sulfur compounds emitted to the atmosphere from natural and anthropogenic sources are an important precursor of acid rain, which seriously damages the environment. Sulfur resides in the atmosphere mainly in the form of gas-phase SO_2 and H_2S as well as sulfate ion SO_4^{2-}.

Sulfur dioxide is a basic precursor of acid rain. Its concentration at the surface level is estimated at $1\,\mu g\,m^{-3}$. The participation of SO_2 in acid rain formation takes place in two ways: through dry deposition onto a wet surface and formation of H_2SO_4 directly in the atmosphere with subsequent deposition either onto land surfaces or in water basins. Sulfur dioxide reacts with water to give sulfuric acid: $SO_2 + H_2O + \frac{1}{2}O_2 \rightarrow H_2SO_4$. These processes are shown in Figure 2.6. SO_2 residence in the atmosphere depends strongly on the means of its removal. As a result of dry deposition, SO_2 is removed from the atmosphere in 7.6 days and its transformation to SO_4^{2-} in 13 days. The rate of dry deposition depends on the type of surface and many other environmental parameters. This rate averages $2\,cm \cdot s^{-1}$ over land and $0.9\,cm\ s^{-1}$ over the ocean. As a result of the combination of the processes of SO_2 removal from the atmosphere its residence can shorten to 4.8 days.

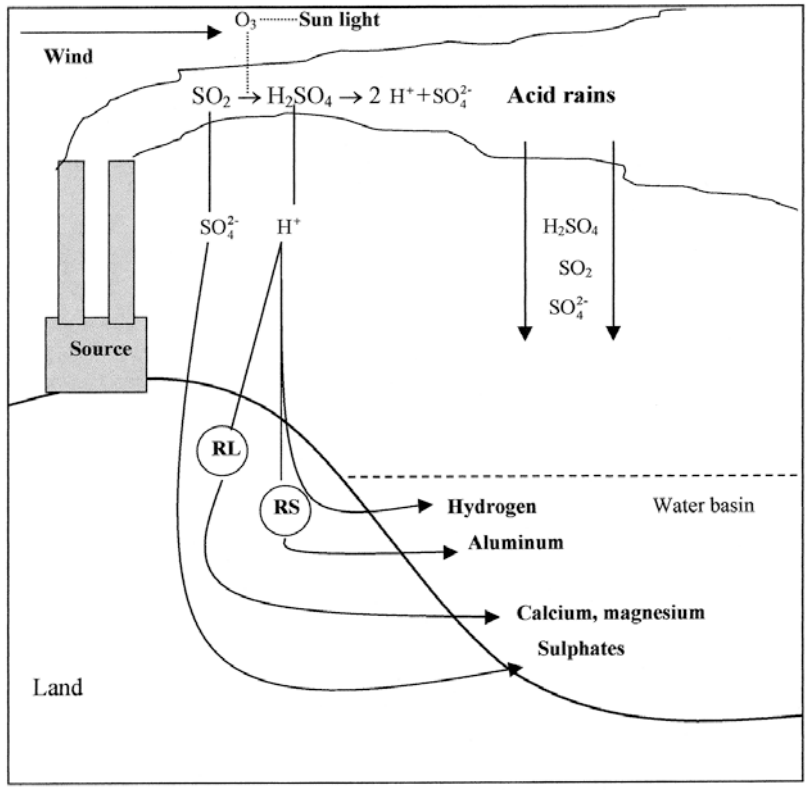

Figure 2.6. A conceptual scheme of the impact of anthropogenic sulfur emissions on the quality of the aquatic medium. Notation: RL, reactions with limestone minerals; RS, reactions with aluminum-containing silicate minerals.

A simplified formula for acid rain is: acid rain $= H_2O + SO_2 + NO_2$. Natural and anthropogenic emissions of SO_2 to the atmosphere are responsible for 60 to 70% of acid rain globally. Deposition from the atmosphere of excessive sulfate is estimated at $360\,Tg \cdot yr^{-1}$ at an average emission rate to the atmosphere of $110\,Tg \cdot yr^{-1}$, with 31% of excessive sulfate in rain water being anthropogenic in origin. On the whole, anthropogenic sources emit to the atmosphere >90% S. These sources are:

- coal burning (coal contains 2–3% S and its burning gives SO_2);
- oil burning and refining (the power of sulfur sources is four to five times lower than that of coal burning);
- ore melting to obtain metals such as copper, nickel, and zinc;
- volcanic eruptions;
- organic decomposition;
- weathering of sulfur-containing rocks ($\sim 15\,Tg \cdot yr^{-1}$);

- input of sulfur to the atmosphere with sea spray ($\sim 45\,\mathrm{Tg \cdot yr^{-1}}$);
- sulfate fertilizers and their subsequent input to the atmosphere with dust ($\sim 10\,\mathrm{Tg \cdot yr^{-1}}$);
- aviation and car engines.

Natural sources of sulfur compounds in the form of hydrocarbons, dimethylsulfide, carbonylsulfide, and methylmercaptan include soils, marshes, forests, volcanoes, the hydrosphere, and agricultural soils. Dimethylsulfide from the surface of the World Ocean reaches the atmosphere and is rapidly oxidized to give sulfates that reside in the atmosphere for no more than 5 days. Available estimates put the sulfur emission of volcanoes annually to the atmosphere from 4 million to 16 million tonnes of sulfides (recalculated for SO_2). Sulfur-containing compounds also form as a result of geothermal activity and the activity of living organisms on land and in water. Rivers bring sulfur to seas and oceans at the rate of $\sim 100\ \mathrm{Tg \cdot yr^{-1}}$. Natural sources of sulfur are rather small. For instance, in the U.S.A. and Canada the emissions of sulfur products from natural sources constitute, respectively, no more than 4 and 18% of total sulfur emissions.

The spectrum of anthropogenic sources of sulfur compounds is diverse and variable because it is present in many minerals such as coal, oil, iron, copper, and other ores. Humankind's use of these minerals leads to sulfur emissions to the atmosphere despite the use of purification devices. The main by-product of industrial processes and fossil fuel burning is sulfur dioxide. For instance, in the U.S.A., SO_2 emissions can be traced to electric power stations 67%, fossil fuel burning 3%, industrial enterprises 15%, transport 7%, and other sources 8%. Globally, these indicators vary strongly both in space and time. For example, in contrast to the U.S.A., electric power stations in Canada emit 20% SO_2, whereas non-ferrous metallurgy emits 43% SO_2. On the whole, in Canada industrial enterprises are the main source of SO_2 (74%). It should be noted that the sources of sulfur in the U.S.A. are responsible for more than 50% of acid rain in Canada, and territories bordering Quebec province get up to 75% of acid rain as a result of SO_2 emissions in the U.S.A. Available estimates put the trans-boundary transport of SO_2 from the U.S.A. to Canada at 3.5 million to 4.2 million tonnes per year.

In most countries, as a consequence of the intense use of petroleum, the problem of acid rain has caused economic problems. Petroleum in the recent past contained sulfur ranging from 150 to 600 ppm. Economic losses because of acid rain forced developed countries to find technologies to reduce the content of sulfur in petroleum. The expected level of 30–50 ppm targeted for 2005 was reached.

The structure of sulfur dioxide emissions is similar in most countries. In Germany, power stations contribute about 90% of the total emissions of sulfur dioxide, while industrial enterprises and transport contribute only 7.5% and 2.5%, respectively. Emissions of sulfur compounds to the atmosphere at high latitudes are clearly seasonal in nature. On reaching the atmosphere from different sources in a given territory, sulfur compounds can be transported by air masses for long distances and deposited in other territories. Knowledge of the spatial distribution

of the concentration of sulfur compounds together with meteorological information should make it possible to predict acid rain.

An expert system that takes into account the totality of models of atmospheric transport of pollutants, and at the same time includes a model of the sulfur cycle in the environment as an independent unit, would make such predictions possible. Of course, there are difficulties here as a result of a limited global database and the absence of some functional descriptions. These difficulties can be overcome using a global simulation model within which the sulfur cycle is parameterized with due regard to the role of the many subsystems of the biosphere and anthropogenic processes. Moreover, inclusion of the sulfur unit in a GSM would broadens its functions, since it is dictated by the dependence of biotic processes on the content of sulfur in biospheric compartments. Available data on the supplies and fluxes of sulfur compounds in the atmosphere, soils, vegetation cover, and hydrosphere would enable mathematical relationships to be formulated to simulate the global sulfur cycle.

Globally, the sulfur cycle is a mosaic of local fluxes of its compounds carried by other elements as a result of water migration and atmospheric processes. The conceptual schemes of global and regional sulfur cycles have been described in detail by many authors (Kondratyev *et al.*, 2006; Krapivin and Kondratyev, 2002; Nitu *et al.*, 2004). However, the available models have been designed for autonomous functioning and application, which does not facilitate their inclusion in a GSM without substantial changes in their parametric spaces. We now offer a solution to this problem.

Sulfur in its non-metallic state is widespread in nature and is a component of global biogeochemical cycles. From the human perspective, sulfur belongs to the group of elements that can negatively affect vital media. The harmful impact of sulfur on the environment is manifested mainly through acid rain. Water basin acidity due to acid rain and subsequent transport of sulfur compounds with the runoff from adjacent lands are manifestations of this impact.

Processes causing the acidification of water basins are mainly connected with anthropogenic sources of sulfur and, of course, other chemical elements such as nitrogen. In the pre-industrial period, the acidity of inland water basins never dropped below $pH = 8$. With the growing anthropogenic impact on the environment, water basin acidity increased with many basins dropping to $pH = 5.7$ in the middle of the last century. At present, in highly industrialized areas natural water basin acidity is about $pH < 5$. The increasing trend of acidity causes serious problems for fish reserve control. Many lakes and rivers in North America and Europe have been excessively acidified, resulting in the aquatic biota in them suffering irreversible changes. For instance, in the U.S.A. (Stoddard *et al.*, 2003) about 4.2% of lakes and 2.7% of river systems are in such a state that their capability to neutralize high acidity naturally is non-existent. The chronic excess of acidification of water basins ($pH < 5.2$) leads to irreversible changes in ecosystems and to a decrease in their survivability.

As seen in Figure 2.6, many factors affect the composition of water, the most important of which being vegetation cover and soil type in the aquatic system's

basin. Therefore, acidity regulation can only be brought about by considering all the factors involved as a complex, which is only possible using numerical models. Experimental technologies cannot be used for this purpose due to the unique character of natural systems. Acid rain is a serious cause of forest damage, especially coniferous forests. As a rule, forests grow in regions that have sufficiently high rainfall and, hence, can get large doses of harmful elements when rainfall turns acid damaging leaves and pine needles and changing the soil composition. At $pH \in [2, 2.6]$ vegetation productivity drops drastically and at $pH \leq 2$ young shoots wither. On the whole, at $pH \in [0.5]$ there is a danger of acid rain and changes to the parameters involved in soil–plant formation. The degree of danger depends on the climatic zone and the type of soil–plant formation. At $pH \geq 5.6$, precipitation is not a threat to the environment.

The soils of most forests have $pH \in [3.2, 5.5]$. The stability of ion exchange processes in the soil is the reason for this interval. It is this stability that preserves the living conditions for the root systems of trees. An excess of cations H^+ in the soil affects the leaching of nutrients while the conversion of insoluble aluminum compounds to soluble ones leads to ion-forming centers being substituted and, as a consequence, external conditions for the root system get seriously compromised.

For global assessment of the role acid rain plays in the environment, a database is needed that can characterize regional pH levels and give the structure of pH-forming processes. Partial databases have been formed in many developed countries, but they are not up to the task of parameterizing the global pattern of acid rain formation. As shown by Safai *et al.* (2004), such data have been collected for India. Using observational data of the rain composition in India for the period 1984–2002, Safai *et al.* (2004) found the content of SO_4 and NO_3 in rain water in the rainy season steadily growing over many regions of India, but the pH level remaining within the alkalinity range. Such data and knowledge of trans-boundary fluxes of sulfur make it possible to calculate pH levels with due regard to the growth of industrial production and development of transport. Another example of database accumulation for acid rain control is an analysis of trends in changes of SO_2 and SO_4^{2-} concentrations in the atmosphere over urban territories of the western and mid-Western regions of the U.S.A. for the period 1990–1999. The important thing here is assessment of the spatial variability of these concentrations (30–42%), which makes it possible to more reliably calculate the parameters of the respective equations in the biogeochemical units of models of atmospheric aerosol transport.

The model of the global sulfur cycle (MGSC) proposed here is a unit of the GSM whose inputs and outputs are compatible with other units of the global model. In contrast to hydrogen, sulfur compounds cannot be attributed to long-lived elements of the biosphere. Therefore, the spatial digitization of the sulfur unit's natural and anthropogenic reservoirs should be planned to reflect the local distributions of sulfur in the vicinity of its sources in such a way as to enable estimation of the intensities of inter-regional fluxes of sulfur compounds. The version of the sulfur unit proposed here, in contrast to known hydrodynamic models of long-distance transport, takes into account the fluxes of sulfur com-

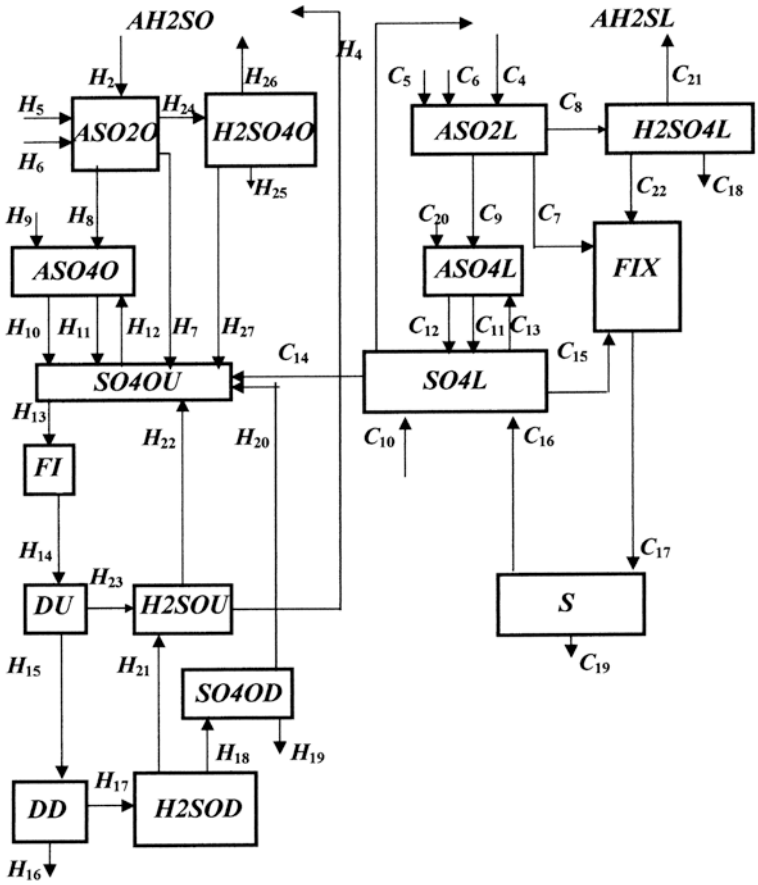

Figure 2.7. The scheme of sulfur fluxes in the environment considered in the MGSC. Notation is given in Table 2.3.

pounds between the hydrosphere, atmosphere, soil, and biota. The model does not consider vertical stratification of the atmosphere. The characteristics of sulfur fluxes over land and oceans averaged vertically are calculated. The spatial digitization of the biosphere and the World Ocean corresponds to a criterion inherent in the GSM. A block scheme of the model of the biogeochemical cycle of sulfur is shown in Figure 2.7, and a description of the fluxes of sulfur compounds is given in Table 2.3. This scheme can be applied to every cell Ω_{ij} of the Earth's surface and every compartment Ω_{ijk} of the World Ocean. The interaction between cells and compartments is organized through the climate unit of the GSM. Therefore, the equations of the sulfur unit lack terms reflecting the dynamic pattern of the spatial transformation of sulfur reservoirs. With due regard to notations assumed in Figure 2.7 and in Table 2.3, the equations describing the balance relationships between the reservoirs of sulfur compounds are written in the form of ordinary differential equations (Krapivin and Kondratyev, 2002).

Table 2.3. Characteristics of land and hydrospheric fluxes of sulfur shown in Figure 2.7. Assessments of fluxes ($mg\,m^{-3}\,day^{-1}$) obtained by averaging over the respective territories.

Sulfur flux	*Land*		*Hydrosphere*	
	Identifier	*Estimate*	*Identifier*	*Estimate*
Volcanic eruptions				
H_2S	C_1	0.018	H_3	0.0068
SO_2	C_5	0.036	H_5	0.0073
SO_4^{2-}	C_{20}	0.035	H_9	0.0074
Anthropogenic emissions				
H_2S	C_2	0.072	H_1	0.00076
SO_2	C_6	0.92	H_6	0.038
SO_4^{2-}	C_{10}	0.47		
Oxidation of H_2S to SO_2	C_4	1.13	H_2	0.3
Oxidation of SO_2 to SO_4^{2-}	C_9	1.35	H_8	0.16
Dry sedimentation of SO_4^{2-}	C_{12}	0.37	H_{11}	0.11
Fallout of SO_4^{2-} with rain	C_{11}	1.26	H_{10}	0.38
Biological decomposition and emission of H_2S into the atmosphere	C_3	1.03	H_4	0.31
Assimilation of SO_4^{2-} by biota	C_{15}	0.41	H_{13}	1.09
Biological decomposition and formation of SO_4^{2-}	C_{16}	1.13	H_{17} (H_{23})	0.43 (0.12)
Sedimentation and deposits	C_{18} C_{19}	0.22 0.11	H_{15} (H_{25}) H_{16} (H_{19})	0.98 (0.036) 0.55 (0.0076)
Wind-driven return to the atmosphere	C_{13}	0.25	H_{12}	0.33
Replenishing sulfur supplies due to dead biomass	C_{17}	0.86	H_{14}	1.1
Assimilation of atmospheric SO_2	C_7	0.46	H_7	0.18
Washing out SO_2 from the atmosphere	C_8	0.27	H_{24}	0.061
River runoff of SO_4^{2-} to the ocean	C_{14}	1.17		
Transformation of gas-phase H_2SO_4 to H_2S	C_{21}	0.018	H_{26}	0.0076
Assimilation of the washed-out part of atmospheric SO_2 by biota	C_{22}	0.036	H_{27}	0.015
Oxidation of H_2S to SO_2 in water medium			H_{18} (H_{22})	0.045 (0.19)
Advection of SO_2			H_{20}	0.38
Advection of H_2S			H_{21}	0.37

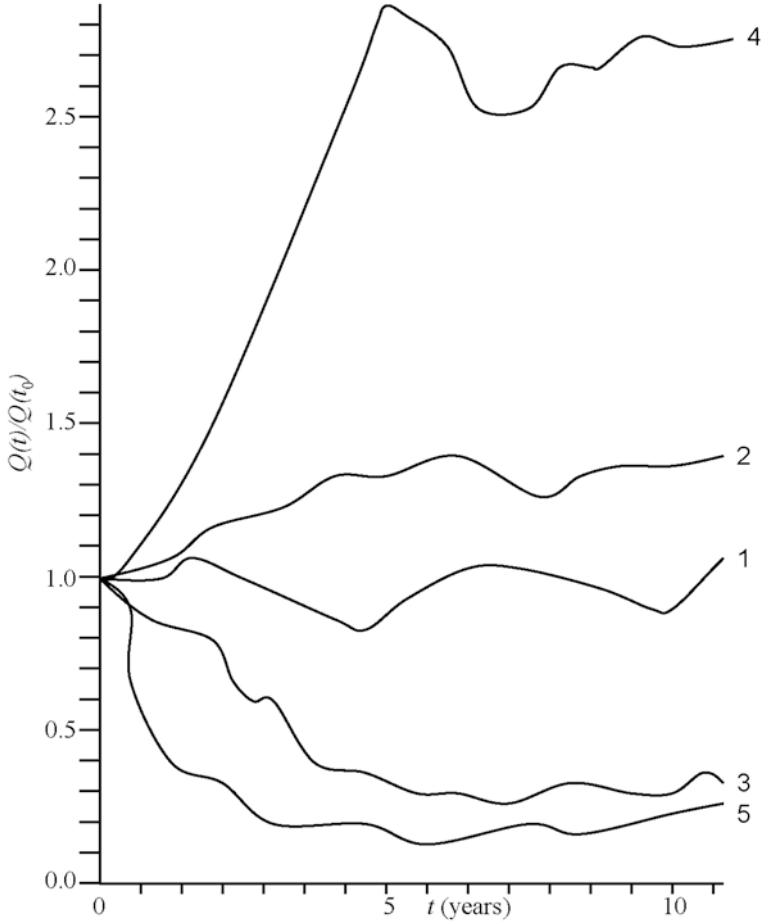

Figure 2.8. Dependence of the dynamics of sulfur concentrations $Q(t)/Q(t_0)$, normalized to initial conditions, averaged over Ω on initial conditions: 1—initial conditions correspond to standard data; 2—reduced by 50%; 3—increased by 50%; 4—reduced by 70%; 5—increased by 70%.

The parameterization accuracy of the GSM sulfur unit, like all units of biogeochemical cycles, is similar to that of other GSM units, and therefore there is no deregulation of the global model, and the stability of results of simulation experiments is ensured. To check this stability, we have undertaken some numerical experiments, taking the parameters of the sulfur unit from Kondratyev *et al.* (2006) and assuming $\Delta\varphi = 4^\circ$, $\Delta\lambda = 5^\circ$, $\Delta z_1 = 10\,\text{m}$, $\Delta z_2 = 100\,\text{m}$. As follows from Figure 2.8, any enhancement of sulfur supplies affects the system's dynamics during the first 2 years, whereas a decrease delays the system's return to a stationary regime for 5 years.

The curves in Figure 2.9 characterize acid rain's dependence on the level of anthropogenic activity. Calculations have shown that the pH value of precipitation

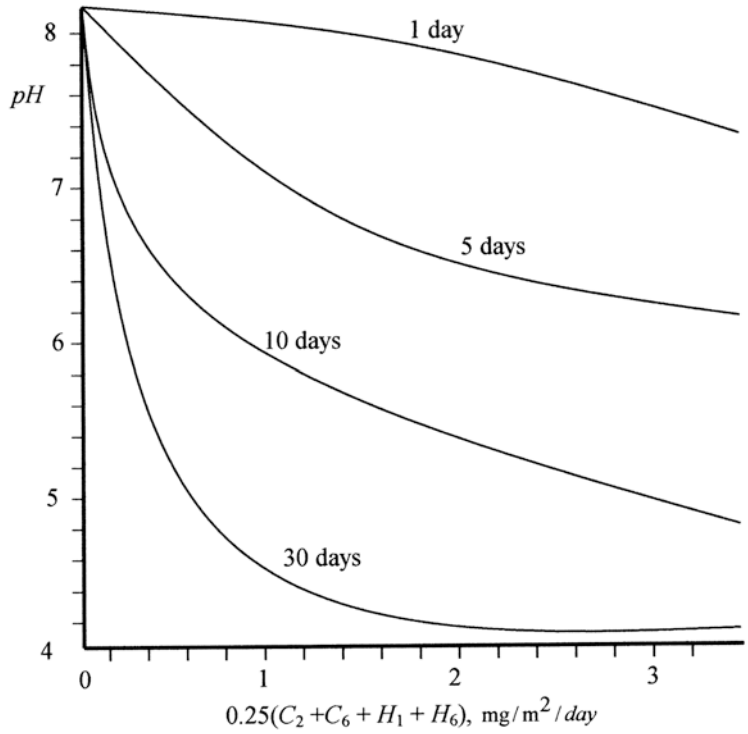

Figure 2.9. Dependence of the average acidity of rain on anthropogenic sulfur fluxes. Change in anthropogenic activity is assumed to be homogeneous in all territories. The curves are labeled with the time that has elapsed since the beginning of the experiment. pH is calculated with the formula $pH = \lg H^+$.

stabilizes, on average, within 30 days from the moment at which anthropogenic emissions of sulfur change. The spatial distribution of the pH of rain with an even increase in fluxes of C_2, C_6, C_{10}, H_1, and H_6 by 0.2% yr^{-1} does not markedly change for 3 years. The ratio of acid rain rates between latitudinal bands 70°–90°N and 70°–90°S remains, on average, at a level of 2.5.

Let us now estimate the contribution of various regions to Arctic pollution. With the stable state of the mean annual concentration of gas-phase H_2SO_4 in the Arctic atmosphere assumed to be 100%, the contributions of countries or territories to the formation of this level are as follows: the U.S.A. 17%, Canada 21%, Europe 37%, and the eastern territory of Russia 25%. These estimates correlate with anthropogenic sulfur fluxes as a result of anthropogenic activity as determined by the relationship of all parameters of the global sulfur cycle. As seen from Figure 2.10, the intensity of biological decomposition in water is distributed non-uniformly, and this means that hydrocarbon production in the oceans is a function of the vertical structure of their ecosystems. For instance, in the Indian Ocean there are two distinct maxima of H_2S production. A weak second

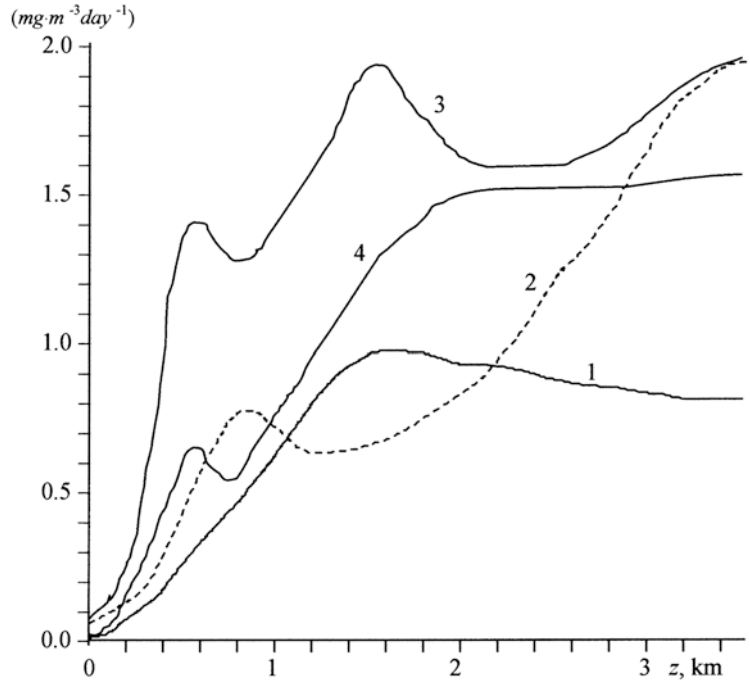

Figure 2.10. Average production of H_2S ($mg\,m^{-3}\,day^{-1}$) in the oceans: 1, Arctic Ocean; 2, Pacific Ocean; 3, Indian Ocean; 4, Atlantic Ocean.

maximum of hydrocarbon production appears at depths of ~1.5 km in the Atlantic Ocean. In other oceans, there is a single maximum of the vertical distribution of H_2S.

Numerical modeling as outlined above shows that reliable assessment of the spatial distributions of pH levels depends on many factors including the accuracy of parameters in equations of the MGSC unit and the form in which the GSM is referenced. To increase the reliability of acid rain forecast, it is necessary to further improve the MGSC unit by including the biogeochemical cycles of other chemicals, such as carbon bisulfide and sulfurous anhydride. By restricting consideration to sulfur dioxide, sulfates, and hydrocarbons in the models of the global sulfur cycle limits the accuracy of these models. Unfortunately, most international and national programs studying the sulfur cycle are confined to these elements.